Elsevier Editorial System(tm) for
Palaeogeography, Palaeoclimatology, Palaeoecology
Manuscript Draft

Manuscript Number: PALAEO9668

Title: Regional Climate and Vegetation Change during Interglacial Events within the mid-Pliocene Warm Period

Article Type: Research Paper

Keywords: Pliocene; Climate; Variability; Interglacial; Orbit; Vegetation

Corresponding Author: Ms. Caroline Louise Prescott,

Corresponding Author's Institution: University of Leeds

First Author: Caroline Louise Prescott

Order of Authors: Caroline Louise Prescott; Aisling M Dolan, PhD; Alan M Haywood, PhD; Stephen Hunter, PhD; Julia C Tindall, PhD; Steven J Pickering, PhD

Abstract: Warm periods in Earth's history can be examined to help understand climate and environmental processes in a warmer-than-modern world. The mid-Pliocene Warm Period (mPWP; 3.264-3.025 Ma) is a recognised valuable target for environmental reconstruction and modelling and the focus of many previous studies. However, the nature of climate and environmental variability on orbital timescales during the mPWP remains poorly constrained. Here, for the first time, we use climate model simulations to analyse mPWP vegetation cover and how this varies between four distinct, and particularly pronounced, interglacial events during the mPWP (Marine Isotope Stages (MIS) G17, K1, KM3 and KM5c)). We also assess climate feedbacks associated with the changes in vegetation. Overall global annual mean surface air temperatures for the studied interglacials are 1.0°C - 1.7°C higher than a comparable Pliocene experiment that uses a modern orbital forcing. Increased spring/summer and reduced autumn/winter insolation in the Northern Hemisphere during MIS G17, K1 and KM3 relative to the modern orbit leads to increased seasonality in temperature and precipitation.

For all interglacials, the climate variability and associated simulated vegetation types are primarily driven by the changed pattern of seasonal insolation. Two of the largest regional responses are seen in North America and continental Eurasia, where forests are replaced by more open-type vegetation (grasslands and shrubland) for interglacials with the most extreme orbital forcing. This trend is amplified through the inclusion of vegetation climate feedbacks, leading to the widespread loss of forest to a degree that cannot be supported by available terrestrial palaeobotanical records. The results demonstrate the importance of examining model performance under a range of palaeoclimate conditions even within the same broad time interval (e.g. mPWP). We propose that further investigation of regional variability in vegetation throughout the mPWP is necessary to examine the validity of model predicted regional climate and vegetation responses.

Suggested Reviewers: Matthew Pound

Senior Lecturer, Geography, University of Northumbria
matthew.pound@northumbria.ac.uk
Matthew Pound is an expert in terrestrial biota and climate, specifically with vegetation reconstructions. He also has some experience and a good understanding of the climate modelling side.

Vanessa Bowman
Palynologist, Palaeo Environments, Ice Sheets and Climate Change team, British Antarctic Survey
vanwma@bas.ac.uk
Vanessa Bowman is an expert in the field of palynology and specialises in reconstructing climate and environments during past warm periods.

Robert S Thompson
Earth Surface Processes, U.S. Geological Survey
rthompson@usgs.gov
Robert Thompson is an expert in Pliocene vegetation. More specifically vegetational response to climate change, and vegetation-land surface impacts climate change.

Dieter Demske
Researcher, Earth Sciences, Freie Universitat Berlin
demske@zedat.fu-berlin.de
Dieter Demske is a palynologist. He is an expert in vegetation reconstruction and the lead author of a paper I have compared my modelling results with in this work.

Pavel E Tarasov
Professor, Earth Sciences, freie universität berlin
ptarasov@zedat.fu-berlin.de
Pavel Tarasov is an expert in vegetation reconstruction and the lead author of a paper compared with the results submitted.

Regional Climate and Vegetation Change during Interglacial Events within the mid-Pliocene Warm Period

[1*]Prescott, C.L., [1]Dolan, A.M., [1]Haywood, A.M., [1]Hunter, S.J., [1]Tindall, J.C and [1]Pickering S.J.

[1]*School of Earth and Environment, University of Leeds, Woodhouse Lane, Leeds, LS2 9JT, UK.*

Corresponding author: C.L.Prescott (js07c2lp@leeds.ac.uk)

Abstract

Warm periods in Earth's history can be examined to help understand climate and environmental processes in a warmer-than-modern world. The mid-Pliocene Warm Period (mPWP; 3.264-3.025 Ma) is a recognised valuable target for environmental reconstruction and modelling and the focus of many previous studies. However, the nature of climate and environmental variability on orbital timescales during the mPWP remains poorly constrained. Here, for the first time, we use climate model simulations to analyse mPWP vegetation cover and how this varies between four distinct, and particularly pronounced, interglacial events during the mPWP (Marine Isotope Stages (MIS) G17, K1, KM3 and KM5c)). We also assess climate feedbacks associated with the changes in vegetation. Overall global annual mean surface air temperatures for the studied interglacials are 1.0°C – 1.7°C higher than a comparable Pliocene experiment that uses a modern orbital forcing. Increased spring/summer and reduced autumn/winter insolation in the Northern Hemisphere during MIS G17, K1 and KM3 relative to the modern orbit leads to increased seasonality in temperature and precipitation.

For all interglacials, the climate variability and associated simulated vegetation types are primarily driven by the changed pattern of seasonal insolation. Two of the largest regional responses are seen in North America and continental Eurasia, where forests are replaced by more open-type vegetation (grasslands and shrubland) for interglacials with the most extreme orbital forcing. This trend is amplified through the inclusion of vegetation climate feedbacks,

leading to the widespread loss of forest to a degree that cannot be supported by available terrestrial palaeobotanical records. The results demonstrate the importance of examining model performance under a range of palaeoclimate conditions even within the same broad time interval (e.g. mPWP). We propose that further investigation of regional variability in vegetation throughout the mPWP is necessary to examine the validity of model predicted regional climate and vegetation responses.

1. Introduction

The mid-Pliocene Warm Period (mPWP), approximately 3.264 to 3.025 million years ago, was the most recent interval in Earth history when global annual mean temperatures are considered to have been higher than the pre-industrial (Haywood et al. 2013a; Dowsett et al. 2012). A continually updated and large palaeoenvironmental reconstruction produced by the Pliocene Research Investigations and Synoptic Mapping (PRISM) project (e.g. Dowsett et al. 1994), in combination with additional proxy studies and modelling investigations, has enabled the mPWP to become a well-studied warm interval in Earth history (Haywood et al. 2013a).

Primarily, the PRISM palaeoenvironmental reconstruction focussed on sea surface temperatures (SST), originally just for the North Atlantic (Dowsett & Poore 1991) before further developing into a global reconstruction which includes vegetation cover. Applying a time slab approach (Dowsett & Poore 1991), the PRISM project reconstructed average interglacial conditions throughout the mPWP and found warming concentrated in the high latitudes, with minimal change in the tropics (Dowsett & Poore 1991; Dowsett et al. 1994; Dowsett et al. 1996).

The PRISM vegetation reconstruction is based on palaeobotanical data; it indicates a warmer and moister climate than today (Salzmann et al. 2008), with the largest differences found in the high latitudes related to a pronounced warming in this region (Thompson & Fleming 1996). The warmer and wetter climate, on average, during the mPWP resulted in a northward shift of the taiga-tundra boundary and a spread of tropical savannahs and woodland in Africa and Australia at the expense of arid deserts (Salzmann et al. 2008).

In order to generate a satisfactory distribution of global vegetation data, the PRISM3 vegetation reconstruction incorporated records from the whole Piacenzian Stage of the Pliocene (~1 million years in duration; Salzmann et al. 2008). The majority of records within the reconstruction are not dated on orbital timescales and could potentially represent interglacial or glacial conditions. However, where it was possible to reconstruct more than one potential biome from an individual locality, the biome representing the warmest climate condition was chosen (Salzmann et al. 2008).

Salzmann et al. (2013) completed a terrestrial data/climate model comparison for the mPWP using a global set of confidence-assessed, proxy-based temperature estimates and biome reconstructions. Their study assesses the performance of eight climate models that participated in the Pliocene Model Intercomparison Project (PlioMIP). A cold bias (up to 10°C) in mean annual surface air temperatures was found in models in the northern hemisphere, particularly north of 30°N. Haywood et al. (2013a) also found that models underestimate the magnitude of temperature change over land and ocean in the northern hemisphere high latitudes. Data-model mismatches were greatest (up to 18°C) in northern Russia and North Alaska, however, the reason for this is unclear. Modelled surface air temperatures (SAT) appeared to be too high in the tropical zone, however, due to limited proxy data availability over this area this signal is less robust.

In published mPWP data-model comparison (DMCs), the ~ 1million year PRISM reconstruction has been compared to model simulation that represent a short time interval, therefore comparing two distinct realisations of the Pliocene (e.g. Dowsett et al., 2012, Salzmann et al., 2013). This discrepancy could explain some part of data-model inconsistencies such as the greater degree of higher latitude warming seen in the PRISM reconstruction compared to climate model results (Lunt et al. 2012; Haywood et al. 2013b). It could also lead to model agreement with data wherein reality this is not justified. The average of warm terrestrial climate signals would have been produced by multiple changing and interacting forcing mechanisms (such as orbital forcing and CO_2 concentration) and cannot be considered a reconstruction of terrestrial environmental conditions that existed at one particular moment in time during the mPWP (Haywood et al. 2013b).

While the PRISM3 vegetation reconstruction is for the whole of the Piacenzian Stage, published vegetation records are available that provide an indication of terrestrial climate variability through the mPWP. For example, the joint pollen and marine faunal study for Japan, by Heusser and Morley (1996), found temperatures varying between dry and humid conditions on top of an overall drying and cooling trend. Wu et al. (2011) also found a general drying trend over the interior of central Asia reconstructed from sporopollen records.

The Willis et al. (1999) sequence from Pula Maar showed significant fluctuations in vegetation between boreal and temperate forest, as well as dust data, thought to directly reflect changes in continental aridity and vegetation. Cyclic fluctuations between dry and humid periods were found in sediments dated 3.7 to 1.7 Ma in North West Africa that can be tied to distinct marine isotope stages (Leroy & Dupont 1994). The vegetation record from the James Bay Lowland in Canada fluctuates between deciduous and boreal forests in time with the benthic oxygen isotope records (Gao et al. 2012a). Tarasov et al. (2013) derived biome reconstructions based on pollen results from Lake El'gygytgyn in north-east Russia and found millennial-scale vegetation changes in the region that corresponded well with alternating cool and warm marine isotope stages during the mPWP. The record from Lake Baikal in south-central Siberia found short term intervals of climate deterioration controlling forest development and advances open vegetation that overlay long term trends of cooling during the Pliocene (Demske et al. 2002).

While mPWP climate conditions are stable relative to the glacial cycles of the Pleistocene epoch (2.6 million to 11,700 years ago), variability in the benthic oxygen isotope stack of Lisiecki and Raymo (2005; LR04) over the mPWP suggests that the impact of orbital forcing on the climate remained substantial. For the purpose of this paper we define a Pliocene interglacial as any isotope excursion which results in more negative $\delta^{18}O$ (benthic oxygen isotope) values than the Holocene average. A previous climate modelling study by Prescott et al. (2014) assessed the nature of climate variability around two interglacial events (Marine Isotope Stage (MIS) K1 and MIS KM5c) in the mPWP, which had different characteristics of orbital forcing. Prescott et al. (2014) demonstrated that orbitally-forced changes in surface air temperature during these interglacial events were substantial and therefore could contribute to uncertainties in the validity of terrestrial data/model comparison. However,

Prescott et al. (2014) did not incorporate additional feedbacks associated with changes in orbital forcing (such as ice-sheet evolution and vegetation change) and therefore could have under or overestimated the difference in climate between these interglacial events.

Here we continue to investigate interglacial climate variability within the mPWP through examining the four most negative benthic oxygen isotope excursions. These are MIS G17, K1, KM3 and KM5c (Fig. 1) as seen in the LR04 benthic oxygen isotope stack (Lisiecki & Raymo 2005).These 'super-interglacial' events (Raymo et al., 2009) have been targeted by the PLIOMAX (Pliocene Maximum Sea Level) project in a multidisciplinary approach to investigate Pliocene sea level high stands.

In this study we analyse and compare the effect of orbital forcing on terrestrial climate and vegetation during these four super-interglacial events within the mPWP. Changes in vegetation are important as they can impact the physical properties of the land surface (e.g. surface albedo, surface roughness) and influence the absorption of energy through changing albedo, as well as the alteration of energy splitting between sensible and latent heat (Foley et al. 2000; Brovkin et al. 2002). Vegetation taken as a prescribed 'boundary condition' does not account for vegetation changes due to climate and the resultant feedback on climate. The addition of vegetation climate feedbacks in response to orbital forcing may be particularly important in the high latitudes where data model disagreement has been noted (Salzmann et al., 2013).

Here we use a general circulation model (GCM) with a dynamic vegetation component to address the following questions:

1. What is the impact of orbital forcing on biome predictions for the four largest interglacial events in the mPWP and how do they vary from each other?
2. How does the addition of dynamic vegetation alter the distribution of plant functional types, the biome reconstruction and the climatological response to orbital forcing?
3. How do model simulations compare with high resolution vegetation data reconstructed at each interglacial? Can the model reproduce the variation in vegetation seen in the proxy data?

2. Methods

2.1 Model description

In this study we use the general circulation model HadCM3 coupled with either the dynamic vegetation model Top-down Representation of Interactive Foliage and Flora Including Dynamics (TRIFFID) or with a prescribed vegetation scheme. Therefore, in this study two versions of the Met Office Surface Exchanges Scheme (MOSES) are used. Simulations with the dynamic vegetation model use the MOSES2.1 land surface scheme, and those with prescribed vegetation use MOSES1 in order to remain consistent with previous studies (e.g. Bragg et al., 2012; Prescott et al. 2014).

We also use the BIOME4 model, which is an offline coupled biogeography and biogeochemistry model that simulates natural vegetation types (biomes) driven by HadCM3 climatology. This allows us to compare predicted biomes for all simulations directly to the Salzmann et al (2008) vegetation reconstruction (PRISM3 vegetation reconstruction).

2.1.1 HadCM3

A comprehensive description of the UK Met Office Hadley Centre Coupled Model Version 3 (HadCM3) used in this study is available in Gordon et al. (2000) and Cox et al. (1999). HadCM3 has been widely used for palaeoclimate modelling, with simulations of the Last-Glacial Maximum and Mid-Holocene climates as well as the mPWP (Braconnot et al. 2007) and deeper time. HadCM3 is a dynamically and thermodynamically coupled atmosphere, ocean and sea ice model. The resolution of the atmosphere component is 2.5 degrees in latitude by 3.75 degrees in longitude which translates to a grid spacing of 278 km by 417 km at the equator. The atmosphere model is composed of 19 layers with a time step of 30 minutes. The representation of evaporation includes the dependence of stomatal resistance on temperature, vapour pressure and CO_2 concentration. The ocean model has a spatial resolution of 1.25 by 1.25 degrees with 20 layers. The sea ice model contains parameterisation of ice drift and leads (Cattle et al. 1995) with a simple thermodynamic scheme.

2.1.2 MOSES Land surface scheme

175 The simulations included in this study use two different version of the Met Office Surface
176 Exchange Scheme (MOSES; versions 1 and 2.1), a land surface scheme that calculates
177 exchanges of heat, moisture, momentum and CO_2 between the surface and atmosphere
178 (Essery et al. 2003). While there are other, less significant enhancements, MOSES1 mainly
179 differs from MOSES2.1 by using effective parameters to calculate a single surface energy
180 balance for each grid box, while MOSES 2.1 includes a tile model (Essery et al. 2003; Best et
181 al. 2006). In MOSES2.1, the grid boxes which were previously treated as whole are now
182 characterised as mosaics of distinct surface types. Separate surface temperatures, shortwave
183 and longwave radiative fluxes, sensible and latent heat fluxes, ground heat fluxes, canopy
184 moisture contents, snow masses and snow melt rates are computed for each surface type or
185 tile in a grid box. The different surface types recognised are broadleaf and needle leaf trees,
186 C_3 and C_4 grasses, shrub, inland water, bare soil and ice. A grid box can be made of any
187 combination of surface types apart from those classified as land-ice. The fractions of surface
188 types within each grid box are modelled by TRIFFID (Falloon et al. 2011).

189 *2.1.3 TRIFFID vegetation model*

190 The dynamic global vegetation model (DGVM) TRIFFID computes the structure and
191 distribution of six plant functional types (broadleaf tree, needle leaf tree, C_3 grass, C_4 grass,
192 shrub and bare soil). The areal coverage, leaf index and canopy height of each plant type is
193 updated using a carbon balance approach where vegetation change is directed by net carbon
194 fluxes calculated within the MOSES 2.1 land surface scheme (Cox 2001). The carbon fluxes are
195 derived using the coupled photosynthesis-stomatal conductance model developed by Cox et
196 al. (1998) that utilises existing models of leaf-level photosynthesis in C_3 and C_4 plants (Collatz
197 et al. 1991; Collatz et al. 1992). Climate and CO_2 drive the resulting rates of photosynthesis
198 and plant respiration. Each plant functional type (PFT) is updated over a grid box (normally
199 every 10 model days) based on competition from other plant types, modelled using the Lotka-
200 Volterra approach and the net carbon available. Soil carbon is increased by litter fall and is
201 returned to the atmosphere by microbial respiration at a rate based on temperature and soil
202 moisture (Cox 2001).

203 TRIFFID can be run in equilibrium and dynamic mode. The equilibrium mode is coupled
204 asynchronously to the atmosphere model, with accumulated carbon fluxes passing though

MOSES2 (Cox 2001). Using the equilibrium method has been shown to be successful in producing equilibrium states for the slowest variables in the model (for example, soil carbon and forest cover) by offline tests. This is often followed by carrying out a dynamic run in order to allow faster varying components (such as grasses) to reach equilibrium with seasonally varying climate (Cox 2001). The modes used in this study are detailed in the methodology of this paper.

2.1.4 BIOME4

BIOME4 is a coupled carbon and water flux model that predicts vegetation distribution, structure and biogeochemistry, and accounts for interactions among these (Kaplan 2003). The model is driven by long term averages of monthly mean temperature, sunshine and precipitation. The model also requires information on soil texture and depth to determine water holding capacity and percolation rates. There are twelve plant functional types (PFTs) each with a small number of bioclimatic limits in order to determine whether or not it could be present in each grid cell. The seasonal maximum leaf area index (LAI) that maximises net primary production (NPP) for each PFT is calculated based on a daily time step simulation of soil water balance and monthly processes based calculations of canopy conductance, photosynthesis, respiration and phenological state (Kaplan 2003; Haxeltine & Prentice 1996). The PFT with the highest NPP is selected as the dominant plant type. In order for the biome to be identified, the PFTs are ranked according to a set of rules based on the computational biogeochemical variables, including NPP, LAI and mean annual soil moisture (Kaplan 2003). This ranking in each grid cell controls the selection of one of twenty seven biomes.

2.2 Boundary conditions and experimental design

In this paper we present results from ten climate model simulations (Table 1). Four experiments were run with HadCM3 based on experimental designs from the PlioMIP project (Haywood et al. 2010; Bragg et al. 2012) using PRISM3D boundary conditions (Dowsett et al. 2010) and the MOSES 1 land surface scheme with prescribed vegetation from Salzmann et al. (2008). While the PlioMIP project used modern orbit, here we have performed simulations for MIS G17, K1, KM3 and KM5c interglacials using orbital parameters derived from the Laskar et al. (2004) astronomical solution. For these interglacials the specific orbit used in the

234 simulations represent the peak of the interglacial according to the LR04 benthic oxygen
235 isotope stack. An additional four experiments were run with the same set up but this time in
236 conjunction with the dynamic vegetation model TRIFFID and the MOSES 2.1 land surface
237 scheme. All eight experiments were run for five hundred years with the final 100 years used
238 to calculate the required climatological averages. Table 1 details the simulations included in
239 this study.

240 The experiments using TRIFFID were run using equilibrium mode (where TRIFFID is coupled to
241 the atmospheric model, with accumulated carbon fluxes passing through MOSES 2.1 (Cox
242 2001) for the first 50 years and subsequently run in dynamic mode for the remainder of the
243 simulation (450 years)). All simulations were subsequently run through BIOME4 in order to
244 compare biome types between those run with prescribed vegetation and those with dynamic
245 vegetation.

246 When running BIOME4 a standard anomaly method was used, this subtracts the control
247 climate simulation from the palaeo simulation and adds the resulting 'anomaly' to the present
248 day baseline climatology. This approach compensates for first order bias in the HadCM3
249 control simulations (Kaplan 2003). Due to the lack of sufficient observational data this method
250 could not be employed over Antarctica, the resulting biome predictions in this region are
251 generated using absolute climatological values from HadCM3 rather than using an anomaly
252 method.

253 Haywood et al. (2013b) show that the peak of MIS KM5c is characterised by a near modern
254 orbital forcing within a period of low eccentricity and low precession (Laskar et al. 2004;
255 Prescott et al. 2014). In this study therefore, when examining changes in the climatology in
256 the simulations of the four interglacials, KM5c is considered as the control climate experiment.

257

258 **3. Results – Climatological response to orbital forcing**

259 *3.1 Pliocene interglacial climate differences*

260 We have simulated four interglacials within the mPWP using prescribed (HadCM3 MOSES1)
261 and dynamic vegetation models (HadCM3 MOSES2.1 coupled with TRIFFID). All interglacials

using both versions of the model are warmer than the pre-industrial control experiments (range of 18.05°C to 19.45°C global annual mean temperatures). Our experiments for KM5c are similar to previous mPWP climate simulations that have modern orbit (in terms of the large-scale features of temperature and precipitation change; Haywood et al. 2013a), due to the near modern orbital configuration during MIS KM5c (3.205 Ma). The other interglacials are between 0.5°C and 0.7°C warmer as a global annual mean average than KM5c for the prescribed vegetation experiments and between 0.5°C and 0.6°C warmer for the dynamic vegetation experiments (Table 1). Global annual mean total precipitation rate increases are between 0.036mm/day and 0.049mm/day for prescribed and 0.011mm/day and 0.033mm/day for dynamic vegetation experiments (Table 1). Experiments incorporating dynamic vegetation are on average 0.725°C warmer, as a global annual mean average, than those using prescribed, which may be attributable to either general differences in the model or the feedbacks on climate associated with the implementation of dynamic vegetation. Broadly all regional patterns of temperature and precipitation change are enhanced in the MOSES2 experiments relative to MOSES1 for each of the studied interglacials. The detailed climate response associated with each interglacial will be described alongside the vegetation (biome and PFT) predictions below.

3.1 MOSES1 prescribed vegetation experiments

The large-scale features of surface temperature change and precipitation (relative to the pre-industrial experiment) are seen in all of the four experiments (Figs. 2d and 2h), however the degree of change in Plio-G17^{Prescribed}, Plio-K1^{Prescribed}, Plio-KM3^{Prescribed} is intensified (Fig. 2a-c, 2e-g). The dominant features include progressive warming in the high latitudes of both hemispheres, a greater degree of surface warming over the land versus the oceans, cooling over tropical Africa and India, related to increases in precipitation and associated evaporative cooling, and an enhanced di-pole pattern in the North Atlantic (related to a change in the mode of sinking/deep-water formation, which has been observed previously using this version of the model (see Prescott et al., 2014)).

A key difference between experiments Plio-G17^{Prescribed}, Plio-K1^{Prescribed}, Plio-KM3^{Prescribed} and Plio-KM5c^{Prescribed} is the generally reduced seasonal range of temperatures in the Southern Hemisphere versus the increased seasonal range of temperatures in the Northern Hemisphere

(particularly over land). This is understandable based on the changes in orbital forcing shown in Figure 1 (b-e).

The four interglacial experiments (Plio-G17^{Prescribed}, Plio-K1^{Prescribed}, Plio-KM3^{Prescribed} and Plio-KM5c^{Prescribed}) with prescribed vegetation were run through the offline vegetation model BIOME4 to classify them into different biomes for comparison purposes. Figure 3a shows the PRISM3 vegetation reconstruction from Salzmann et al. (2008) for reference. As the PRISM3 vegetation reconstruction is prescribed in the model, the subsequent biome reconstructions are in some respects constrained to the PRISM3 dataset. Any differences are due to inconsistencies between the simulated Pliocene climate and the original vegetation reconstruction (PRISM3) or are a function of the climate response to the orbital forcing imposed.

There are regional differences in biome distribution when compared to the PRISM3 reconstruction. In all four interglacial peaks South Africa is dominated by shrubland and desert instead of forest and woodland in the PRISM3 reconstruction. All interglacials show a larger expanse of grassland in North America and Asia, as well as enhanced desert over Australia and a loss of trees to shrubland in South America. Plio-KM5c^{Prescribed} predicts the most similar biome reconstruction to PRISM3. This is to be expected as this interglacial has the least difference from modern orbital conditions (Haywood et al. 2013b; Prescott et al., 2014).

3.2 MOSES2.1 Dynamic vegetation experiments

In order to understand how the addition of dynamic vegetation can impact the climate response to orbital forcing, as well as to further understand the changes seen in vegetation distribution, we investigate annual and seasonal SAT and precipitation changes in the four interglacials (Fig. 4) alongside the changes in the simulated vegetation (Fig. 5 and 3f-3i).

The annual SAT differences (the interglacials minus the Plio-KM5c^{Dynamic} control) show a similar pattern to the Plio-KM5c^{Dynamic} minus Pre-Ind^{Dynamic} (Fig. 4d) but with a greater magnitude of change. Interglacials Plio-G17^{Dynamic} and Plio-KM3^{Dynamic} present greater high latitude warming compared to Plio-KM5c^{Dynamic} than Plio-K1^{Dynamic}. For Plio-G17^{Dynamic} warming of 2°C is

predicted, and in Plio-KM3^{Dynamic} warming reaches 3.5°C at the high latitudes (60°N – 90°N) relative to the Plio-KM5c^{Dynamic} control experiment. Patterns of temperature change such as warming in the high latitudes and tropical cooling are seen in all of the interglacials (when differenced to Plio-KM5c^{Dynamic}) and are generally consistent with the simulations using prescribed vegetation (Fig. 2).

TRIFFID's predictions of PFTs are described in order to better understand the differences between the interglacials due to orbital changes and dynamic vegetation feedbacks (Fig 5). Here we discuss the results in relation to how they are different to the Plio-KM5c^{Dynamic} control broken down into different regional responses.

Africa

In Plio-KM5c^{Dynamic} there is 80-90% broadleaf forest over southern and central Africa with 100% bare soil (desert) in North Africa, Arabia and the west coast of southern Africa. The forest and bare soil are separated by a thin band of grassland at approximately 15°N.

Plio-K1^{Dynamic} and Plio-KM3^{Dynamic} show 80 – 90% increase of broadleaf trees across southern North Africa. This replaces bare soil and the grasses therefore pushing the boundary between forest and grassland northwards. Plio-G17^{Dynamic} shows this same pattern but broadleaf increase is over a much smaller area and is less intense. In the Plio-K1^{Dynamic} interglacial Southern Africa shows a loss of 80-100% broadleaf to bare soil and grassland, with Plio-KM3^{Dynamic} showing a slight loss of broadleaf and the occurrence of grasses.

North America

Plio-KM5c^{Dynamic} has a mixed forest of broadleaf and needle leaf trees in North America with the highest percentage of broadleaf trees predominately focussed in the northern continental interior and South East America and Mexico. The rest of America, Canada and Greenland (outside of the ice sheet) is dominated by needle leaf trees.

Plio-G17^{Dynamic}, Plio-K1^{Dynamic} and Plio-KM3^{Dynamic} share similar spatial changes in vegetation over North America. They show 30–50% more broadleaf trees over Canada and Alaska and a reduction of the same PFT of 30-40% in Central and Eastern America in comparison to Plio-KM5c^{Dynamic}. This increase of broadleaf is associated with a decrease of needle leaf trees over

the same areas. There are also areas of increasing shrub (up to 60%) to the west of America replacing needle leaf trees.

South America

There is forest of up to 90% broadleaf trees over most of South America in the Plio-KM5c^{Dynamic} control simulation. Over the remaining areas, predominantly the interior of Northern Brazil, there are areas of 85% grassland and along the east coast of Brazil, 100% bare soil. Chile and southern Argentina are dominated by needle leaf trees.

Over South America, the differences in PFTs compared to Plio-KM5c^{Dynamic} seen in interglacial peaks Plio-G17^{Dynamic}, Plio-K1^{Dynamic} and Plio-KM3^{Dynamic} are minor. However, over Brazil, Plio-G17^{Dynamic} and Plio-KM3^{Dynamic} show increases in broadleaf trees (between 20% and 60%), whereas Plio-K1^{Dynamic} shows a decrease of up to 60% over the southern East coast of Brazil.

Eurasia

Plio-KM5c^{Dynamic} shows Eurasia largely covered in forest, including 70% broadleaf forest over Spain and southwestern Europe. Central Siberia and areas of southern Asia (e.g. South China and Indonesia) have broadleaf forest concentrations reaching 95%. The remaining areas of Northern Eurasia have 50 - 75% of needle leaf trees. Grassland can be seen in India and in central Asia south of the simulated forest line. There are shrubs found in small areas throughout Asia, particularly in the north-eastern region.

All three interglacials exhibit localised increases in broadleaf trees in northern Eurasia, however, the dominant response is up to 60% decline in needle leaf trees that are replaced by grasses (20% increase) and shrubs (up to 60% increase). The largest difference in PFTs for the interglacials is in the Northern region of India where there is a 100% reduction in bare soil, replaced by grassland and broadleaf trees.

Australia

Australia in the Plio-KM5c^{Dynamic} control experiment includes large areas of broadleaf forest to the north and east of the country, grassland through the centre, surrounded by shrubland and bare soil in the south east.

Plio-G17^{Dynamic}, Plio-K1^{Dynamic} and Plio-KM3^{Dynamic} all predict a reduction in grassland in central Australia which is replaced with broadleaf forest to the north and shrub to the south. There is also a shared pattern of associated with a 60% increase shrub in southern Australia replacing bare soil. Plio-K1^{Dynamic} has a slightly more pronounced pattern of change, comprising a 60% reduction in broadleaf forest along the north east coastline with grassland growing instead.

Antarctica

Plio-KM5c^{Dynamic} and Plio-G17^{Dynamic} predict mainly shrub and grassland over non-glaciated regions of Antarctica with small areas of bare soil. The largest changes predicted over Antarctica are within the Plio-K1^{Dynamic} interglacial. Experiment Plio-K1^{Dynamic} suggests that all grasses and shrubs on the Antarctic margins are replaced by bare soil. Experiment Plio-KM3^{Dynamic} has a similar predicted vegetation distribution with a smaller area of increased bare soil and grassland.

The addition of dynamic vegetation does not impact the climate response in a simple, uniform way. There are some areas where adding vegetation causes positive feedbacks, for example, increases the temperature signal (be that, positive or negative) and also examples of negative feedbacks where this signal is reduced with the addition of dynamic vegetation. There is enhanced warming over central South America (5°C anomaly in Plio-K1^{Dynamic}) and southern Africa (up to 10°C anomaly in Plio-K1^{Dynamic}) compared to the Plio-KM5c^{Dynamic} control. This is due to feedbacks through partial replacement of forest with grasses in South America, and with grasses, shrubs and bare soil in southern Africa. The occurrence of more open types vegetation (in Africa and South America; Fig. 5) is caused by the orbitally forced warming in these areas (in Plio-K1^{Prescribed}; Fig. 2b) and enhanced by decreases in evapotranspiration (not shown). This is linked with a decrease in precipitation in the Plio-K1^{Prescribed} experiment (Fig. 2f). The larger temperature change seen in central Africa is a result of a positive feedback between vegetation and surface temperature brought about through the northward shift of the Sahara desert and its replacement with broadleaf forest and grasses (Fig. 4 and Fig. 5).

Over India, bare soil is replaced with broadleaf forest and grasses and this change amplifies the local cooling demonstrated in the prescribed vegetation experiments. The largest positive feedback effect is seen in Plio-K1^{Dynamic} over Antarctica. This area shows higher albedo (not

shown) due to snow cover and temperatures of -3.5°C less than Plio-KM5c^{Prescribed}. When using dynamic vegetation the simulated albedo over Antarctica is increased further due to the total loss of vegetation (shrub and grass) and its replacement with bare soil leading to further cooling (Plio-K1^{Dynamic} is 9°C colder than Plio-KM5c^{Dynamic}).

In the prescribed vegetation experiments we demonstrate a trend towards more open vegetation in Eurasia (Fig. 3b-e), linked primarily to changes in insolation patterns. The differences in vegetation (in terms of PFT, Fig. 5) are enhanced further by positive feedbacks in dynamic vegetation (reduction of precipitation, evapotranspiration and soil moisture associated with the loss of forest).

There are however, also areas of cooling seen in the MOSES2 simulations when run with dynamic vegetation that are not seen in the simulations run solely with changing orbital forcing and prescribed vegetation. For example, coastal northeast Brazil shows a cooling of approximate 5°C when compared to Plio-KM5c^{Dynamic} (in all interglacials; Fig. 4a-c). This appears to be due to an orbitally driven vegetation switch from bare soil and grasses to broadleaf forest and therefore increasing evapotranspiration (and an increase of the latent heat flux). Coupling the simulations to a dynamic vegetation model also induces a cooling of 2°C (in all interglacials) on the coastline of South Australia. This temperature change occurs with the replacement of bare soil and grass with shrub, and is associated with an increase of evaporative cooling in this region (not shown).

There is a negative feedback on high latitude warming with the introduction of dynamic vegetation, especially in two interglacials (Plio-KM3^{Dynamic} and Plio-G17^{Dynamic}) that show greater high latitude warming than Plio-KM5c^{Dynamic}. Broadleaf trees in the Arctic have twice the albedo and 50 – 80% greater evapotranspiration rates when leafed-out than their evergreen needle leaf counterparts (Swann et al. 2010). More broadleaf forest replacing needle leaf along the Arctic coast would have a cooling effect due to increased evapotranspiration, moderating the high northern latitude warming signal.

The cause and effect of the simulated climate response to orbit and vegetation changes is complicated, as in addition to introducing a dynamic vegetation model, two different land surface schemes were used in this study. Where the inclusion of dynamic vegetation has made

the terrestrial areas generally warmer, this could be arguably due to the use of MOSES2 (over MOSES1), which in previous analysis has been found to be a warmer model. However, we can suggest that the areas where the introduction of dynamic vegetation simulates an increased cooling, to be solely a signal from vegetation feedbacks.

3.3 MOSES2.1 Dynamic Large scale biome changes (BIOME4)

The four interglacial experiments (Plio-G17^{Dynamic}, Plio-K1 ^{Dynamic}, Plio-KM3 ^{Dynamic} and Plio-KM5c ^{Dynamic}) with dynamic vegetation were run through the offline vegetation model BIOME4 to classify them into different biomes for comparison purposes.

Patterns of biome distribution appears similar between the four interglacials (using dynamic vegetation). All have expanded grassland over Asia and North America, with Eastern Europe/Scandinavia predominantly showing temperate deciduous forest. They all show large areas of desert in northern and southern Africa, however three experiments (Plio-G17^{Dynamic}, Plio-K1 ^{Dynamic}, Plio-KM3 ^{Dynamic}) show smaller desert areas with more xerophytic shrubland than Plio-KM5c ^{Dynamic} over central Australia. The Arctic coastline has predominantly evergreen taiga/montane forest. South America has tropical forest biome to the north and shrubland and mixed forest types to the south.

There are detailed differences between the BIOME4 reconstructions for the dynamic vegetation experiments. For example, across central Africa Plio-K1^{Dynamic} and Plio-KM3^{Dynamic} show a band of deciduous forest, whereas Plio-G17^{Dynamic} and Plio-KM5c^{Dynamic} are more dominated by tropical savannah and shrubland biomes. In Plio-KM5c^{Dynamic}, taiga montane forest reaches the Arctic coastline and stretches latitudinally across north Asia. The other three interglacials also have taiga montane forest in this region but covering a smaller area. In experiments Plio-K1^{Dynamic} and Plio-KM3^{Dynamic} the band of forest across the coast is broken and pushed north by grassland which can reach the Arctic coast of eastern Asia. North America shows a similar pattern, with evergreen taiga/montane forest again being pushed north by grasslands which in Plio-K1^{Dynamic} and Plio-KM3^{Dynamic} reaches the northern Canadian coastline. Arid desert regions in Australia shrink in Plio-G17^{Dynamic} and Plio-KM3^{Dynamic}, whereas Plio-

461 KM5c^{Dynamic} and Plio-K1^{Dynamic} show a distribution which is similar to the PRISM3
462 reconstruction of desert in this region.

463 In summary, these results show the effect of using dynamic vegetation in climate modelling
464 studies especially when looking at time slices with orbital forcing very different from modern
465 orbital forcing. The BIOME4 output for Plio-KM5c^{Dynamic} is the most similar to the PRISM3
466 reconstruction due to the stable and near modern orbital forcing. The other three interglacials
467 run with dynamic vegetation show a very different terrestrial environments to Plio-
468 KM5c^{Dynamic} (and the PRISM3 reconstruction). The biomes are more stratified latitudinally and
469 are less heterogeneous with large areas of grass in the northern hemisphere mid to high
470 latitudes.

471

472 **4. Discussion**

473 The exploration of discrete interglacial events within the mPWP was investigated in Prescott
474 et al. (2014), which looked at both the MIS K1 and KM5c interglacial peaks and demonstrated
475 that the two events are different in nature in terms of their climatology (Prescott et al., 2014).
476 Here we continue in a similar vein, with the incorporation of two more Pliocene interglacial
477 events (MIS G17 and KM3) to build a fuller picture of mPWP interglacial variability, but with
478 the addition of incorporating dynamic vegetation. We focus our discussion on addressing the
479 importance of orbitally driven changes in seasonality as a driver for regional land cover
480 response, and the validity of model predictions with regard to the available regional
481 palaeobotantical data.

482 *4.1 How important is the effect of orbitally-driven seasonality changes for regional land cover*
483 *response?*

484 The simulated surface air temperatures in Figure 2 shows notably large increases in seasonal
485 range, in relation to the Plio-KM5c^{Prescribed} control simulation, this is due to obliquity and
486 precession altering the seasonal distribution of insolation (Timm et al. 2008). The high
487 obliquity (Fig. 1) of MIS K1 and G17 causes greater warming simulated relative to modern in
488 the high northern latitudes in these interglacials. For all three interglacials, the larger

amplitude of the Northern Hemisphere seasonal signal is forced by both the higher eccentricity (Fig. 1), when compared to MIS KM5c, and the perihelion (point of time where the Earth is closest to the sun) falling during the boreal spring (MIS G17) and summer (MIS K1 and KM3).

Given the robust demonstration of increased seasonality in all simulations, there is a need to understand the seasonal response of temperature in relation to predicted vegetation. For example, the cooling over Antarctica in Plio-K1^{Prescribed} is due to a large insolation reduction (of up to 100 Wm^{-2}; Fig. 1) over the Southern Hemisphere during the summer months that is not seen to the same extent in the other interglacials. The similarities seen between all the interglacials such as northern hemisphere high latitude warming are caused by increases of up to 95 Wm^{-2} in the spring/summer months.

Changes in the seasonality of surface temperature and precipitation response is especially amplified in simulations run with dynamic vegetation (Fig. 4). In these experiments, the Northern Hemisphere shows a enhanced seasonality in all three interglacials compared to the Plio-KM5c^{Dynamic} control. While this is seen most strongly on land due to the low heat capacity of land versus the oceans, the oceans also show the same signal. This is most clearly expressed in Plio-K1^{Dynamic} and Plio-KM3^{Dynamic} due to the largest seasonal differences in orbital driven incoming insolation (Fig, 1).

The larger seasonal range (colder autumn/winters and warmer spring/summers) over the Northern hemisphere coincides with the reduction of forest seen in both BIOME4 output and TRIFFID PFTs in favour of more open vegetation over Eurasia, which is where we see the largest vegetation change.

The colder temperatures in winter over North America/Eurasia do not reduce winter precipitation for MIS K1, G17 and KM3 compared to Plio-KM5c (in both the prescribed and dynamic vegetation simulations). Total precipitation rates for MIS K1, G17 and KM3 increase compared to KM5c during spring in large areas of Eurasia in experiments using prescribed vegetation. However, this is not the case for the same experiments run using dynamic vegetation. During the boreal summer (JJA) large areas of Eurasia receive either the same or less precipitation than the KM5c experiments, even though summer surface temperatures

increase substantially. This reduced seasonal surface moisture availability can affect the seasonal patterns of warming through changes in latent heat flux, and decreased deeper soil moisture availability favouring grass/shrub occurrence over trees (Fig. 4). Grasses have an intense but shallow root system using water from upper soil layers whereas trees roots access deeper soil moisture (Ward et al. 2013). Winter precipitation is critical to recharge deeper soil layers for trees to access (Schwinning et al. 2015), and this process would be especially important in a scenario where summer temperatures increase due to a change in seasonality. Therefore, in these results the warmer spring/summers and lack of associated increase in winter/summer precipitation favours the simulation of grass rather than trees in our model (Figs. 3 and 5). The reduction in available soil moisture in the deepest soil layer (on average 308 mm less in all 4 interglacials than the pre-industrial annual mean, and a decrease to 327 mm less in winter) is seen most acutely in the dynamic vegetation simulations. Given that soil moisture and temperature are fundamental drivers in both TRIFFID (Cox, 2001) and BIOME4 (Haxeltine and Prentice, 1996; Kaplan, 2003) in the prediction of vegetation types, this drying of soil provides a partial explanation for the large-scale tree retreat in Eurasia and North America.

Additionally, the higher summer temperatures seen over Eurasia and North America favours the existence of grass in the BIOME4 model. In BIOME4, through the identification of the 2 most successful PFT's and their sustainable LAI, each model grid cell is assigned a biome (Haxeltine & Prentice 1996). The look up table used within the BIOME4 model uses a value of 21°C as a maximum warm monthly mean temperature for boreal evergreen and deciduous trees to grow. The simulated mean temperature of the warmest month in our HadCM3 results is higher than the maximum used in BIOME4 for forest to grow. When this parameter is changed within BIOME4, the forest/grass boundary moves southwards depending on the maximum warm monthly mean temperature which is chosen (not shown). It appears that this empirical threshold in BIOME4 is partly why trees are replaced with grasses in all experiments for MIS K1, KM3 and G17.

BIOME4 simulates the vegetation distribution that is in equilibrium with a particular climate and atmospheric CO_2 concentration (Haxeltine & Prentice 1996), it does not incorporate migration or successional processes which increases the uncertainty in the results. For

548 prediction of rapidly changing climate response, BIOME4 is able to suggest the general
549 direction and maximum extent of change to be expected but this may be oversimplified.
550 Whereas BIOME4 integrates both biogeochemical processes and a biogeographical
551 description of vegetation, TRIFFID includes these processes as well as their dynamical links to
552 the atmospheric system (Quillet et al. 2010).

553 We therefore use TRIFFID, a DGVM to treat the land cover as an interactive element in order
554 to ascertain the magnitude of vegetation feedbacks from orbitally forced changes in
555 seasonality and the variability between interglacials in the mPWP. TRIFFID separates the
556 vegetation into PFT according to the physical response to climate conditions and runs
557 interactively with the climate model, therefore enabling vegetation feedbacks that are not
558 possible when solely running the climate through BIOME4 without TRIFFID enabled.

559 When considering large scale vegetation changes predicted by TRIFFID, the decline of forest
560 to more open field vegetation (i.e. the combination of grasses, shrubs and bare soil) over Asia
561 represents a significant change in vegetation. This is consistent with the BIOME4 output which
562 shows large expanses of grassland pushing the forest margin northwards in North America
563 and Asia. While BIOME4 predicts temperate grassland across the majority of Asia, TRIFFID
564 shows the main difference to be increasing shrub causing a northward shift in broadleaf tree
565 and an overall reduction of needle leaf at Northern high latitudes. This discrepancy in
566 vegetation distribution is understandable given the differences in the way both models predict
567 vegetation.

568 Given that there are such large changes of vegetation seen over Eurasia in both TRIFFID and
569 BIOME4 we compare these results to published data sites that capture variability in this
570 region.

571

572 *4.2 Looking at specific high resolution records (Lake Baikal and Lake El'gygytgyn , do our*
573 *simulations capture similar variability shown in the data?*

574 At present, the PRISM3 reconstruction represents the whole mPWP and is therefore not
575 directly comparable to the modelling results for each specific interglacial peak directly.

However, vegetation records exist that have high temporal resolution and indicate environmental and climate variability. Our modelled interglacial biomes for the area to the western North America indicate evergreen taiga, in agreement with the pollen record from James Bay (in Canada) (Gao et al. 2012a) . The simulated biomes at the Pula Maar site also show similarities to the vegetation reconstruction, predicting temperate deciduous and conifer forest (Willis et al. 1999) . These areas in the simulated biomes also show large areas of grass which are not seen in the vegetation proxy reconstructions. Heusser and Morley (1996) found the vegetation in Japan, between 4.8 Ma to 2.8 Ma to vary between warm mixed forest and cool conifer and the simulated vegetation shows a large area of warm mixed forest in the four interglacials with some temperate deciduous forest.

While the focus of this study is not to perform a data model comparison, we consider high resolution data where there is information available on variability and where the model simulates large orbitally driven changes indicating model sensitivity. Where there are large changes in the simulated vegetation over North America as well as Asia, there are fewer high resolution records indicating variability in this area. We therefore compare the variability shown in records from Lake El'gygytgyn and Lake Baikal in Siberia with the variability seen in the simulated vegetation over Asia.

Lake El'gygytgyn

Extreme warmth and polar amplification was extrapolated from the record at Lake El'gygytgyn (67.5°, 72°) during the mPWP with a stepped cooling event during the Pliocene-Pleistocene transition (Brigham-Grette et al. 2013) and Arctic summer warmth with forest cover at both warm and cold summer orbits. The vegetation record shows a decline of tree population to an open landscape with the biomization further suggesting that this vegetation transition was not gradual and the region responded rapidly to the warm and cold global climate oscillations seen in LR04 (Tarasov et al. 2013).

Biome reconstructions at Lake El'gygytgyn indicate that the late Pliocene to early Pleistocene can be characterised by six vegetation types- four forest and two open vegetation biomes (Tarasov et al. 2013). The four biomes representing forest found at Lake El'gygytgyn in the Pliocene are either boreal or a mixture of boreal and temperate. The other two biomes are

605 tundra and steppe and are dominated by boreal or arctic herb and shrub communities
606 (Tarasov et al. 2013).

607 The pollen based biome reconstruction at Lake El'gygytgyn (Tarasov et al. 2013) indicate that
608 MIS KM5c coincides with a transition from a cold deciduous biome to a taiga. KM5c also falls
609 within pollen zone 10 in the Andreev et al (2014) record which finds, among others, an
610 increase in Picea (spruce/coniferous evergreen) and Larix (deciduous coniferous) pollen. The
611 pollen based biome reconstruction at KM3 is cool conifer forest (Tarasov et al. 2013) with
612 pollen concentrations showing higher tree pollen counts such as Pinus (Pine), Picea and Larix
613 than KM5c. The reconstructed biome at MIS K1 is on the boundary between cool mixed and
614 cold deciduous forest and tundra (Tarasov et al. 2013). This shift from forest biome to the
615 more open tundra coincides with the pollen assemblage described in Andreev et al. (2014)
616 that describes an increase in shrub pollen (Alnus and Betula) and a decrease in coniferous
617 pollen types. There is both taiga and cool conifer forest at MIS G17 (Tarasov et al. 2013) and
618 pollen concentrations (Andreev et al. 2014) show a decrease in herbs and sedges with high
619 values of Picea increasing at this time.

620 At Plio-KM5c^{Dynamic} the PFTs predicted by TRIFFID are 64% needle leaf tree, 21% shrub and
621 13% grass (remainder bare soil) with BIOME4 simulating cold evergreen needle leaf forest.
622 The surrounding grid squares (up to approximately 600km around Lake El'gygytgyn) show
623 biomes varying between cold evergreen and cool evergreen needle leaf forest, and low and
624 high shrub tundra. The main simulated biome, cold evergreen needle leaf forest, is arguably
625 interchangeable with the taiga, predicted from the pollen data (Tarasov et al. 2013). The cold
626 deciduous biome interpreted from the pollen data, is not represented in the simulated biomes
627 at or around Lake El'gygytgyn in our modelling results, additionally no broadleaf trees
628 predicted by TRIFFID. The biome simulated for Plio-KM3^{Dynamic} is cold evergreen needle leaf
629 forest over Lake El'gygytgyn with cool conifer forest interpreted from the pollen data. The
630 PFTs predicted by TRIFFID also show 65% needle leaf trees. At Plio-K1^{Dynamic} BIOME4 simulates
631 cold evergreen needle leaf forest, with biomes of temperate grassland, temperate deciduous
632 and cool mixed forest simulated in the surrounding grid squares. The pollen based biome
633 reconstruction shows cool mixed and cold deciduous forest moving to a tundra biome. For
634 this interglacial the simulation of forest biome types matches well with the data, although, the

simulated temperate grassland prediction is not seen in the pollen based biome reconstruction. In contrast to BIOME4 simulating grassland, TRIFFID predicts 23% shrub at this site and 12% grass. This is the highest shrub percentage simulated of the interglacials with the interpretation of the pollen based biome to be tundra. For Plio-G17^{Dynamic} BIOME4 simulates cold evergreen needle leaf forest with cool evergreen needle leaf forest and cool mixed forest predicted in the grid squares around. The pollen based biome reconstruction shows taiga and cool conifer forest, indicating consistency with the modelling results. TRIFFID simulated PFTs also predict 67% Needle leaf trees (highest of the simulated interglacials) and a drop to 19% shrub (from Plio-KM3^{Dynamic}).

Lake Baikal

Lake Baikal is situated in the continental interior of north-eastern Eurasia (53°,108°), proxies suggest it was located at the boundary between different vegetation zones during the Pliocene with shifts in distribution of coniferous forests, steppe and mountain vegetation. There is an overall cooling trend between the warm early Pliocene and the onset of Northern Hemisphere Glaciation shown by the reduction of broadleaf trees throughout the record with periods of open vegetation interpreted to have been cool, dry conditions (Demske et al., 2002).

After MIS M2 and leading up to KM5c, the proxy derived vegetation reconstruction suggests a gradual increase in spruce/hemlock forests due to an increase in precipitation. Around the KM5c event (between 3.26 and 3.18 Ma) the record indicates a decrease in forests and the spread of boreal taxa such as birches and dwarf shrubs. KM5c has the highest pollen percentage of shrubs and herbs of the four interglacials in the pollen reconstruction of Demske et al. (2002). The vegetation data around KM5c are interpreted as moist spruce/hemlock (tsuga) forests with ferns occurring under cooler conditions at high altitudes, with the drier forest types and steppe communities at lower elevations (Demske et al., 2002). This corresponds to a macro fauna assemblage in West Siberia reconstructing drier and/or cooler conditions (Zykin 1995).

Around KM3 there are large fluctuations in spruce (picea) abundances and pine (pinus) forests begin to appear in the record leading to a reduction of spruce/hemlock forest. There is evidence of a severely dry interval five thousand years after KM3 (3.150 Ma) with low palaeo-temperatures. Open vegetation (Artemisia) spread between KM3 and K1, with further expansion of open vegetation and dry steppe continuing to increase after K1 (at 3030). There is an overall low pollen count for forest types at K1 with a relatively high shrub and grass pollen concentrations when compared to KM3 and G17. The pollen reconstruction at G17 shows a development of mixed coniferous forest with a specific increase in hemlock indicating a return to warmer conditions (Demske et al., 2002).

There are several major differences between simulated PFTs for Plio-KM5c^{Dynamic} in the Lake Baikal region and the Demske et al (2002) pollen record. Unlike Plio-KM3^{Dynamic}, Plio-K1^{Dynamic} and Plio-G17^{Dynamic}, no shrub is predicted for Plio-KM5c^{Dynamic} and there are high percentages of broad and needle leaf trees (57% and 30% respectively). In contrast, while the pollen record contains a high percentage of spruce pollen at MIS KM5c, the highest percentage of shrub pollen is also seen at this point of the four interglacials.

Demske et al. (2002) suggest that broadleaf forests were suppressed in the lead up to and during the M2 event, with the vegetation still recovering from this cool glacial period at KM5c. The simulations presented in this study are climate snapshots of the interglacials and so this transient recovery from the glaciated M2 event is not represented which could account for the large discrepancy in shrub pollen percentage. In contrast, the simulated PFTs at Plio-KM3^{Dynamic} and Plio-K1^{Dynamic} predict no broadleaf or needle leaf trees, instead predicting, high shrub percentages (~60%) with the remaining vegetation simulated as grass. Reconstructed shrub/herb pollen is low at KM3 but increases shortly after at 3.150 Ma. This increase in open vegetation from 3.150 to 3.030 Ma encapsulates K1 interglacial, which has the highest percentage of simulated shrub plant functional type. The pollen reconstruction indicates a recovery of forest after this period of open vegetation seen around K1, while the simulated plant functional types also show an increase of broadleaf and needle leaf forest (24% and 9%) at Plio-G17^{Dynamic}. The highest percentage of plants simulated at Plio-G17^{Dynamic}, however is still shrub which is not seen in the pollen reconstruction.

692 The simulated biome for all four interglacials is temperate grassland, whereas the vegetation
693 reconstructed at Lake Baikal finds little grass pollen. Analysis of the biomes simulated around
694 Lake Baikal indicate the presence of temperate deciduous broadleaf forest and temperate
695 xerophytic shrubland south of Lake Baikal at 42°N and 45°N for all the simulations.

696 In general, the simulated vegetation is more similar to the Lake El'gygytgyn record than Lake
697 Baikal, where in the simulated Asian continental interior a large expanse of grassland is
698 predicted but not seen in the record. If we look to the TRIFFID output, however, the prediction
699 of shrubs instead of grass is closer to the data which interprets the vegetation to be open
700 steppe.

701 The degree to which the regional patterns of vegetation change shown in our model results,
702 truly reflect what really happened during the four interglacial events in question is difficult to
703 ascertain at the current time. There are no global compilations of the vegetation distribution
704 for the four specific intervals studies and limitations in dating and age control may make
705 attributing a vegetation data point to any of these four events challenging. Regardless, we
706 have tried to compare the variability seen in the simulations to the variability seen in the
707 reconstructed pollen data. The Lake El'gygytgyn record, which has especially variable pollen
708 based biome reconstruction, shows similar level of changes between the interglacials in the
709 simulated biomes. Lake Baikal however, at a biome level shows no variability in the simulated
710 vegetation. The TRIFFID output better reflects the changes in vegetation in the pollen record
711 but still simulates a generally poor representation of this record.

712 In general, the mPWP vegetation proxy data records present a fluctuating climate that swings
713 between annual climate signal of warm-wet (forest), and cool-dry (steppe) (Heusser & Morley
714 1996; Willis et al. 1999; Leroy & Dupont 1994; Gao et al. 2012). Whereas our model results for
715 the interglacials show a more warm and dry signal, especially in the northern hemisphere
716 where there are warmer summers of up to 14°C difference to control summer temperatures
717 as well as cooler winters (up to 5°C cooler).

718 Salzmann et al. (2013) found a significant data-model mismatch with models being too cold
719 by 11.8°C at Lake Baikal when preforming a DMC with HadCM3, while also taking bioclimatic
720 range and temporal variability into account. We would not therefore expect these simulations

of the specific interglacials to necessarily have a good representation of the pollen reconstruction seen in Demske et al. (2002). Although, the simulated continental interior over Asia appears to show a drying of the vegetation across all the interglacials which is generally seen in the data moving into the Pleistocene. The SAT temperature of Plio-KM5c^{Dynamic} is a closer match to the Lake Baikal is of 4.5°C. This is due in part to using MOSES2 which is, in general, a warmer land surface model, but using the M1 model the mismatch is 9.8°C. Annually the temperatures are still too cold even with the new land surface scheme.

Recent palaeoclimate modelling studies Loptson et al. (2014) and Hunter et al. (2013) both using HadCM3L coupled with TRIFFID, describe a model dry bias (associated with TRIFFID) within their results. Here, the predicted biomes also appear to reflect a dry bias but further investigation shows this loss of trees to grassland in the northern hemisphere is due to an increase of seasonality driven principally by changes in the orbital forcing. The hotter spring and summers combined with colder autumn and winters appears to favour grass/shrub vegetation types in our simulations (Haxeltine & Prentice 1996).

The large data-model mismatch found at Lake Baikal could also be due to the proxy record not capturing the simulated interglacial peaks we have modelled here. Orbital sensitivity simulations run for the Eocene, (Sloan & Morrill, 1998) also found increased seasonality in the continental temperatures which was not reflected in any proxy records. The study postulates that while this could be due to the simulations incorrectly predicting seasonal cycles, it could also be due to biases in the preservation of complete orbital cycles that prevents the stronger signals being seen in the proxy record (Sloan & Morrill, 1998). While this could also be the case for this study, the magnitude of the data-model mismatch is so large at Lake Baikal that there may be more fundamental issues with the simulations in this area and the Eurasian continental interior. The better match of data-model comparison at Lake El'gygytgyn, which is located on the Asian Arctic coastline also suggests that the mismatch at Lake Baikal could be related to issues associated with modelling continental interiors.

However, regional biases in model representations of Eurasian hydrology in response to orbital forcing have been reported before. For example, Holocene CMIP5 simulations also found drier conditions in Eurasia compared to palaeo observations that indicate this area was wetter than today (Harrison et al. 2015). For the mid-Holocene climate models simulated a

751 significant increase in the summer temperatures in Eurasia, and therefore seasonality,
752 whereas the observations suggest cooler summers (lower seasonality). Temperature biases in
753 the CMIP5 modern simulations were linked to systematic biases in evapotranspiration with an
754 oversimplification of precipitation leading to cold temperature biases (Mueller & Seneviratne,
755 2014; Harrison et al. 2015). Harrison et al. (2015) suggests that models do not produce a
756 sufficient increase in regional precipitation for the mid-Holocene in Eurasia and therefore
757 underestimate evapotranspiration causing higher summer temperatures. Interestingly, a
758 modelling study on future climate change over Siberia using HadCM3 anomalies for a number
759 of future scenarios, coupled to the Siberian BioClimatic model, found the climate to be drier
760 with a reduction in forest replaced by increased steppe as a result of decreased precipitation
761 and increasing temperatures (Tchebakova et al. 2009).

762 Within this study for the Pliocene we see similar issues with the simulated climate to the
763 studies above, increased seasonality, warmer summers with insufficient precipitation,
764 appears to create a scenario where our modelled climate is unable to sustain forest seen
765 consistently in published records of Eurasian vegetation distribution.

766

767 **5. Conclusions**

768 The mid-Pliocene Warm Period (mPWP) is an important interval to investigate the long term
769 response of vegetation patterns to a CO_2 induced warming. However, the nature of vegetation
770 change in response to orbital variability during this interval is poorly constrained.
771 Understanding the nature of orbitally induced vegetation variability is important to
772 understand the Pliocene overall, and in identifying the degree to which climate and vegetation
773 models are able to reproduce the climate states in Earth history.

774 Here we investigate the degree to which orbital forcing drives changes in surface
775 climatological and land cover response and between four of the largest interglacial events
776 within the mPWP. The degree of surface temperature warming and precipitation response
777 regionally is strongly controlled by orbital forcing. This translates into variations in seasonality
778 and moisture availability that can have profound effects on the predictions of land cover
779 regionally. In our study this is clearly expressed in North America and Eurasia where mid-

Pliocene experiments with increased insolation during the northern hemisphere spring/summer and decreased insolation during autumn/winter (compared to a mid-Pliocene scenario with near modern orbital forcing) lead to a climate response and vegetation climate feedbacks that lead to a marked replacement of forest with open types of vegetation. Whilst available higher resolution palaeobotanical data from the Eurasia indicate that variations in the amount of trees versus more open type vegetation is possible between interglacial events in the mPWP, trees remained a dominant feature of the landscape. This suggests that the climate and vegetation response in the region in our model is overestimated, and this conclusion is similar to studies produced for the mid-Holocene, using a variety of climate models, that indicate similar regional biases in climate and predicted vegetation response to orbital forcing.

This highlights the importance of evaluating model predictions using out of sample palaeo tests and underlines the requirement for additional high resolution palynological studies from around the world in order to better quantify the nature of land cover variability during the mPWP and the ability of climate and vegetation models to reproduce geological evidence.

Acknowledgments

All authors acknowledge receipt of funding from the European Research Council under the European Union's Seventh Framework Programme (FP7/2007-2013)/ERC grant agreement no. 278636. We also acknowledge the EPSRC-funded Past Earth Network.

References:

Andreev, A.A. et al., 2014. Late Pliocene and Early Pleistocene vegetation history of northeastern Russian Arctic inferred from the Lake El'gygytgyn pollen record. *Climate of the Past*, 10(3), pp.1017–1039. Available at: http://www.clim-past.net/10/1017/2014/cp-10-1017-2014.html [Accessed July 25, 2015].

Best, M.J., Grimmond, C.S.B. & Villani, M.G., 2006. Evaluation of the Urban Tile in MOSES using Surface Energy Balance Observations. *Boundary-Layer Meteorology*, 118(3), pp.503–525. Available at: http://link.springer.com/10.1007/s10546-005-9025-5 [Accessed August 7, 2014].

Braconnot, P. et al., 2007. Results of PMIP2 coupled simulations of the Mid-Holocene and Last Glacial Maximum – Part 1: experiments and large-scale features. *Climate of the*

Past, 3(2), pp.261–277. Available at: http://www.clim-past.net/3/261/2007/cp-3-261-2007.html [Accessed January 11, 2016].

Bragg, F.J., Lunt, D.J. & Haywood, A.M., 2012. Mid-Pliocene climate modelled using the UK Hadley Centre Model: PlioMIP Experiments 1 and 2. *Geoscientific Model Development Discussions*, 5(2), pp.837–871. Available at: http://www.geosci-model-dev-discuss.net/5/837/2012/gmdd-5-837-2012.html [Accessed July 30, 2014].

Brigham-Grette, J. et al., 2013. Pliocene warmth, polar amplification, and stepped Pleistocene cooling recorded in NE Arctic Russia. *Science (New York, N.Y.)*, 340(6139), pp.1421–7. Available at: http://www.sciencemag.org/content/340/6139/1421.full [Accessed May 29, 2015].

Brovkin, V. et al., 2002. Carbon cycle, vegetation, and climate dynamics in the Holocene: Experiments with the CLIMBER-2 model. *Global Biogeochemical Cycles*, 16(4), pp.86–1–86–20. Available at: http://doi.wiley.com/10.1029/2001GB001662 [Accessed January 10, 2016].

Cattle, H., Crossley, J. & Drewry, D.J., 1995. Modelling Arctic Climate Change [and Discussion]. *Philosophical Transactions of the Royal Society A: Mathematical, Physical and Engineering Sciences*, 352(1699), pp.201–213. Available at: http://rsta.royalsocietypublishing.org/content/352/1699/201.short [Accessed August 27, 2014].

Collatz, G., Ribas-Carbo, M. & Berry, J., 1992. Coupled Photosynthesis-Stomatal Conductance Model for Leaves of C 4 Plants. *Australian Journal of Plant Physiology*, 19(5), p.519. Available at: http://www.publish.csiro.au/view/journals/dsp_journal_fulltext.cfm?nid=102&f=PP9920519 [Accessed July 30, 2014].

Collatz, G.J. et al., 1991. Physiological and environmental regulation of stomatal conductance, photosynthesis and transpiration: a model that includes a laminar boundary layer. *Agricultural and Forest Meteorology*, 54(2-4), pp.107–136. Available at: http://www.sciencedirect.com/science/article/pii/0168192391900028 [Accessed July 16, 2014].

Cox, P., 2001. Description of the TRIFFID dynamic global vegetation model: Hadley Centre Technical Note 24.

Cox, P.., Huntingford, C. & Harding, R.., 1998. A canopy conductance and photosynthesis model for use in a GCM land surface scheme. *Journal of Hydrology*, 212-213, pp.79–94. Available at: http://www.sciencedirect.com/science/article/pii/S0022169498002030 [Accessed August 28, 2014].

Cox, P.M. et al., 1999. The impact of new land surface physics on the GCM simulation of climate and climate sensitivity. *Climate Dynamics*, 15(3), pp.183–203. Available at: http://link.springer.com/10.1007/s003820050276 [Accessed July 30, 2014].

Demske, D., Mohr, B. & Oberhänsli, H., 2002. Late Pliocene vegetation and climate of the Lake Baikal region, southern East Siberia, reconstructed from palynological data. *Palaeogeography, Palaeoclimatology, Palaeoecology*, 184(1-2), pp.107–129. Available at: http://www.sciencedirect.com/science/article/pii/S0031018202002511 [Accessed May 29, 2015].

Dowsett, H. et al., 1994. Joint investigations of the Middle Pliocene climate I: PRISM paleoenvironmental reconstructions. *Global and Planetary Change*, 9(3-4), pp.169–195. Available at: http://www.sciencedirect.com/science/article/pii/0921818194900159 [Accessed July 30, 2014].

Dowsett, H. et al., 2010. The PRISM3D paleoenvironmental reconstruction. *Stratigraphy*. Available at: http://nrl.northumbria.ac.uk/11399/ [Accessed July 30, 2014].

Dowsett, H., Barron, J. & Poore, R., 1996. Middle Pliocene sea surface temperatures: a global reconstruction. *Marine Micropaleontology*, 27(1-4), pp.13–25. Available at: http://www.sciencedirect.com/science/article/pii/037783989500050X [Accessed August 26, 2014].

Dowsett, H.J. et al., 2012. Assessing confidence in Pliocene sea surface temperatures to evaluate predictive models. *Nature Climate Change*, 2(5), pp.365–371. Available at: http://dx.doi.org/10.1038/nclimate1455 [Accessed July 30, 2014].

Dowsett, H.J. & Poore, R.Z., 1991. Pliocene sea surface temperatures of the north atlantic ocean at 3.0 Ma. *Quaternary Science Reviews*, 10(2-3), pp.189–204. Available at: http://www.sciencedirect.com/science/article/pii/027737919190018P [Accessed August 26, 2014].

Essery, R.L.H. et al., 2003. Explicit Representation of Subgrid Heterogeneity in a GCM Land Surface Scheme. *Journal of Hydrometeorology*, 4(3), pp.530–543. Available at: http://journals.ametsoc.org/doi/abs/10.1175/1525-7541(2003)004<0530:EROSHI>2.0.CO;2 [Accessed August 28, 2014].

Falloon, P. et al., 2011. Validation of River Flows in HadGEM1 and HadCM3 with the TRIP River Flow Model. *Journal of Hydrometeorology*, 12(6), pp.1157–1180. Available at: http://journals.ametsoc.org/doi/full/10.1175/2011JHM1388.1 [Accessed August 28, 2014].

Foley, J.A. et al., 2000. Incorporating dynamic vegetation cover within global climate models. *ESA - Ecological Society of America*.

Gao, C. et al., 2012a. Glaciation of North America in the James Bay Lowland, Canada, 3.5 Ma. *Geology*, 40(11), pp.975–978. Available at: http://geology.gsapubs.org/content/40/11/975.abstract [Accessed July 25, 2015].

Gao, C. et al., 2012b. Glaciation of North America in the James Bay Lowland, Canada, 3.5 Ma. *Geology*, 40(11), pp.975–978. Available at:

886 http://geology.gsapubs.org/content/40/11/975.short [Accessed January 10, 2016].

887 Gordon, C. et al., 2000. The simulation of SST, sea ice extents and ocean heat transports in a
888 version of the Hadley Centre coupled model without flux adjustments. *Climate*
889 *Dynamics*, 16(2-3), pp.147–168. Available at:
890 http://link.springer.com/10.1007/s003820050010 [Accessed July 30, 2014].

891 Harrison, S.P. et al., 2015. Evaluation of CMIP5 palaeo-simulations to improve climate
892 projections. *Nature Climate Change*, 5(8), pp.735–743. Available at:
893 http://www.nature.com/doifinder/10.1038/nclimate2649 [Accessed June 20, 2016].

894 Haxeltine, A. & Prentice, I.C., 1996. BIOME3: An equilibrium terrestrial biosphere model
895 based on ecophysiological constraints, resource availability, and competition among
896 plant functional types. *Global Biogeochemical Cycles*, 10(4), pp.693–709. Available at:
897 http://doi.wiley.com/10.1029/96GB02344 [Accessed May 21, 2015].

898 Haywood, A.M. et al., 2013. Large-scale features of Pliocene climate: results from the
899 Pliocene Model Intercomparison Project. *Climate of the Past*, 9(1), pp.191–209.
900 Available at: http://www.clim-past.net/9/191/2013/cp-9-191-2013.html [Accessed July
901 30, 2014].

902 Haywood, A.M. et al., 2013. On the identification of a pliocene time slice for data-model
903 comparison. *Philosophical Transactions of the Royal Society A: Mathematical, Physical*
904 *and Engineering Sciences*, 371(2001).

905 Haywood, A.M. et al., 2010. Pliocene Model Intercomparison Project (PlioMIP): experimental
906 design and boundary conditions (Experiment 1). *Geoscientific Model Development*, 3(1),
907 pp.227–242. Available at: http://www.geosci-model-dev.net/3/227/2010/gmd-3-227-
908 2010.html [Accessed July 30, 2014].

909 Heusser, L.E. & Morley, J.J., 1996. Pliocene climate of Japan and environs between 4.8 and
910 2.8 Ma: A joint pollen and marine faunal study. *Marine Micropaleontology*, 27(1-4),
911 pp.85–106. Available at:
912 http://www.sciencedirect.com/science/article/pii/0377839895000534 [Accessed May
913 21, 2015].

914 Hunter, S. et al., 2013. Modelling equable climates of the Late Cretaceous: Can new
915 boundary conditions resolve data-model discrepancies? *Palaeogeography,*
916 *Palaeoclimatology, Palaeoecology*. Available at: http://eprints.whiterose.ac.uk/80053/
917 [Accessed January 11, 2016].

918 Kaplan, J.O., 2003. Climate change and Arctic ecosystems: 2. Modeling, paleodata-model
919 comparisons, and future projections. *Journal of Geophysical Research*, 108(D19),
920 p.8171. Available at: http://doi.wiley.com/10.1029/2002JD002559 [Accessed April 15,
921 2015].

922 Laskar, J. et al., 2004. A long-term numerical solution for the insolation quantities of the

923 Earth. *Astronomy and Astrophysics*, 428(1), pp.261–285. Available at:
924 http://dx.doi.org/10.1051/0004-6361:20041335 [Accessed August 28, 2014].

925 Leroy, S. & Dupont, L., 1994. Development of vegetation and continental aridity in
926 northwestern Africa during the Late Pliocene: the pollen record of ODP site 658.
927 *Palaeogeography, Palaeoclimatology, Palaeoecology*, 109(2-4), pp.295–316. Available
928 at: http://www.sciencedirect.com/science/article/pii/0031018294901813 [Accessed
929 May 21, 2015].

930 Lisiecki, L.E. & Raymo, M.E., 2005. A Pliocene-Pleistocene stack of 57 globally distributed
931 benthic δ 18 O records. *Paleoceanography*, 20(1), p.n/a–n/a. Available at:
932 http://doi.wiley.com/10.1029/2004PA001071 [Accessed July 10, 2014].

933 Loptson, C.A., Lunt, D.J. & Francis, J.E., 2014. Investigating vegetation–climate feedbacks
934 during the early Eocene. *Climate of the Past*, 10(2), pp.419–436. Available at:
935 http://www.clim-past.net/10/419/2014/cp-10-419-2014.html [Accessed January 11,
936 2016].

937 Lunt, D.J. et al., 2012. On the causes of mid-Pliocene warmth and polar amplification. *Earth
938 and Planetary Science Letters*, 321-322, pp.128–138. Available at:
939 http://www.sciencedirect.com/science/article/pii/S0012821X12000027 [Accessed May
940 28, 2015].

941 Prescott, C.L. et al., 2014. Assessing orbitally-forced interglacial climate variability during the
942 mid-Pliocene Warm Period. *Earth and Planetary Science Letters*, 400, pp.261–271.
943 Available at: http://www.sciencedirect.com/science/article/pii/S0012821X1400332X
944 [Accessed July 14, 2014].

945 Quillet, A., Peng, C. & Garneau, M., 2010. Toward dynamic global vegetation models for
946 simulating vegetation–climate interactions and feedbacks: recent developments,
947 limitations, and future challenges. *Environmental Reviews*, 18(NA), pp.333–353.
948 Available at: http://www.nrcresearchpress.com/doi/abs/10.1139/A10-016 [Accessed
949 January 11, 2016].

950 Raymo, Maureen E. Hearty, P., De Conto, R., O'Leary, M., Dowsett, H.J., Robinson, M.M.,
951 Mitrovica, J.X., 2009. PLIOMAX: Pliocene maximum sea level project. *PAGES News*,
952 p.Vol. 17. pp 58–59. Available at: http://www.pages-
953 igbp.org/download/docs/newsletter/2009-
954 2/Special_section/science_highlights/Maureen_2009-2(58-59).pdf [Accessed August 28,
955 2014].

956 Salzmann, U. et al., 2008. A new global biome reconstruction and data-model comparison
957 for the Middle Pliocene. *Global Ecology and Biogeography*, 17(3), pp.432–447. Available
958 at: http://doi.wiley.com/10.1111/j.1466-8238.2008.00381.x [Accessed July 30, 2014].

959 Salzmann, U. et al., 2013. Challenges in quantifying Pliocene terrestrial warming revealed by
960 data–model discord. *Nature Climate Change*, 3(11), pp.969–974. Available at:

961 http://dx.doi.org/10.1038/nclimate2008 [Accessed August 15, 2014].

962 Sloan, L.C., Crowley, T.J. & Pollard, D., 1996. Modeling of middle Pliocene climate with the
963 NCAR GENESIS general circulation model. *Marine Micropaleontology*, 27(1-4), pp.51–
964 61. Available at: http://www.sciencedirect.com/science/article/pii/0377839895000631
965 [Accessed May 20, 2015].

966 Swann, A.L. et al., 2010. Changes in Arctic vegetation amplify high-latitude warming through
967 the greenhouse effect. *Proceedings of the National Academy of Sciences of the United*
968 *States of America*, 107(4), pp.1295–300. Available at:
969 http://www.pnas.org/content/107/4/1295.short [Accessed July 16, 2014].

970 Tarasov, P.E. et al., 2013. A pollen-based biome reconstruction over the last 3.562 million
971 years in the Far East Russian Arctic – new insights into climate–vegetation relationships
972 at the regional scale. *Climate of the Past*, 9(6), pp.2759–2775. Available at:
973 http://www.clim-past.net/9/2759/2013/cp-9-2759-2013.html [Accessed July 25, 2015].

974 Tchebakova, N.M., Parfenova, E. & Soja, A.J., 2009. The effects of climate, permafrost and
975 fire on vegetation change in Siberia in a changing climate. *Environmental Research*
976 *Letters*, 4(4), p.045013. Available at: http://iopscience.iop.org/article/10.1088/1748-
977 9326/4/4/045013 [Accessed March 16, 2016].

978 Thompson, R.S. & Fleming, R.F., 1996. Middle Pliocene vegetation: reconstructions,
979 paleoclimatic inferences, and boundary conditions for climate modeling. *Marine*
980 *Micropaleontology*, 27(1-4), pp.27–49. Available at:
981 http://www.sciencedirect.com/science/article/pii/0377839895000518 [Accessed July
982 29, 2014].

983 Timm, O. et al., 2008. On the definition of seasons in paleoclimate simulations with orbital
984 forcing. *Paleoceanography*, 23(2), p.n/a–n/a. Available at:
985 http://doi.wiley.com/10.1029/2007PA001461 [Accessed January 11, 2016].

986 Willis, K.J., Kleczkowski, A. & Crowhurst, S.J., 1999. 124,000-year periodicity in terrestrial
987 vegetation change during the late Pliocene epoch. , 397(6721), pp.685–688. Available
988 at: http://dx.doi.org/10.1038/17783 [Accessed July 25, 2015].

989 Wu, F. et al., 2011. Extended drought in the interior of Central Asia since the Pliocene
990 reconstructed from sporopollen records. *Global and Planetary Change*, 76(1-2), pp.16–
991 21. Available at: http://adsabs.harvard.edu/abs/2011GPC....76...16W [Accessed July 25,
992 2015].

993 Zykin, V., 1995. Changes in environment and climate during early Pliocene in the southern
994 West-Siberian Plain. *… AND GEOPHYSICS C/ …*. Available at:
995 https://scholar.google.co.uk/scholar?q=Environmental+climate+changes+West+Siberia
996 n+Plain+pliocene+zykin+1995&btnG=&hl=en&as_sdt=0%2C5#0 [Accessed January 11,
997 2016].

Figures:

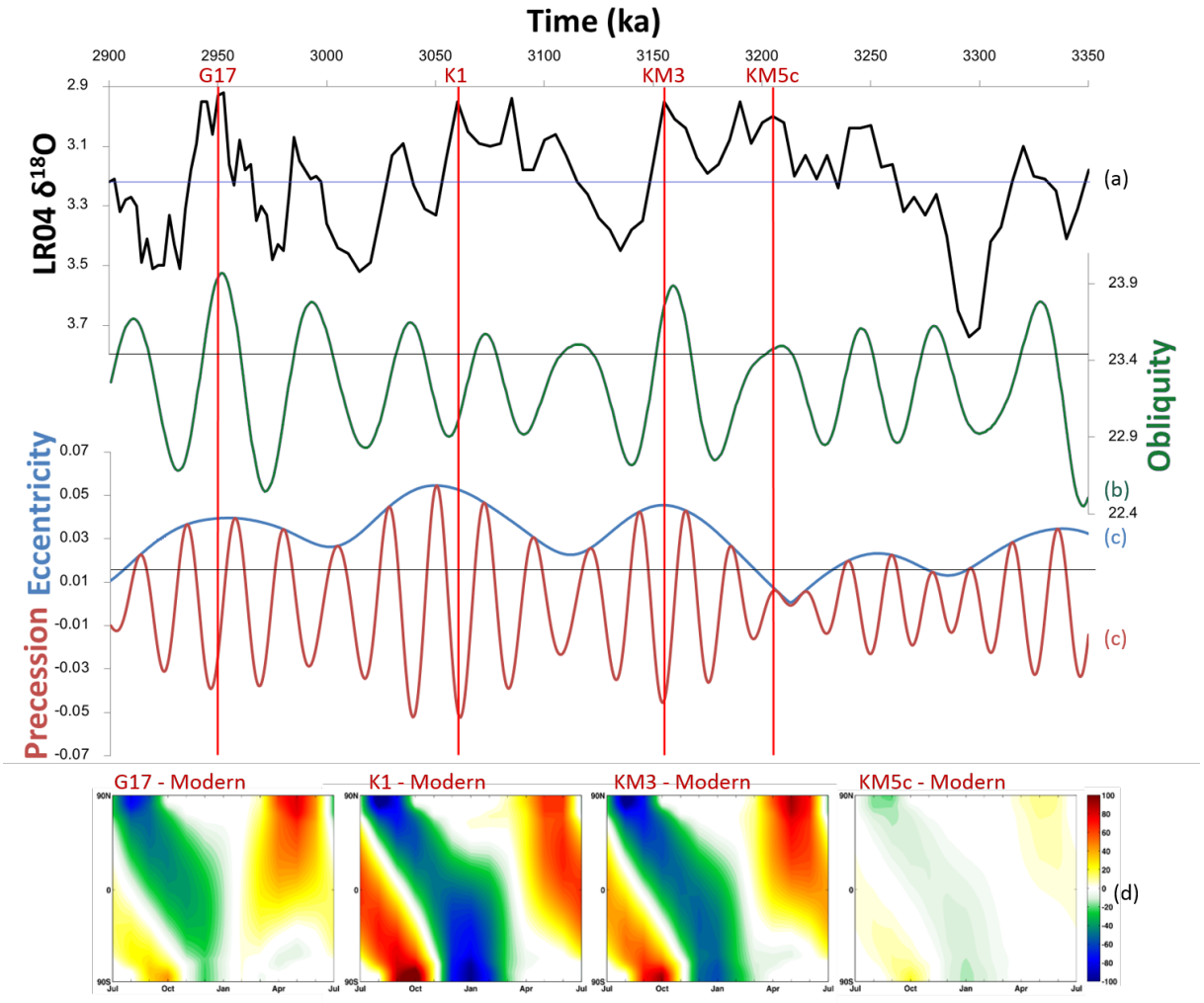

Figure 1. Marine isotope stages G17, K1, KM3 and KM5c plotted on (a) the benthic isotope record of Lisiecki and Raymo (2005). (b) Obliquity, (c) eccentricity, precession as derived from the astronomical solution of Laskar et al. (2004). Black horizontal lines show modern orbit with blue horizontal line showing the Holocene oxygen isotope average. (e) Incoming short wave radiation flux derived from HadCM3 (Wm^{-2}) for MIS G17 minus modern; MIS K1 minus modern, MIS KM3 minus modern; MIS KM5c minus modern.

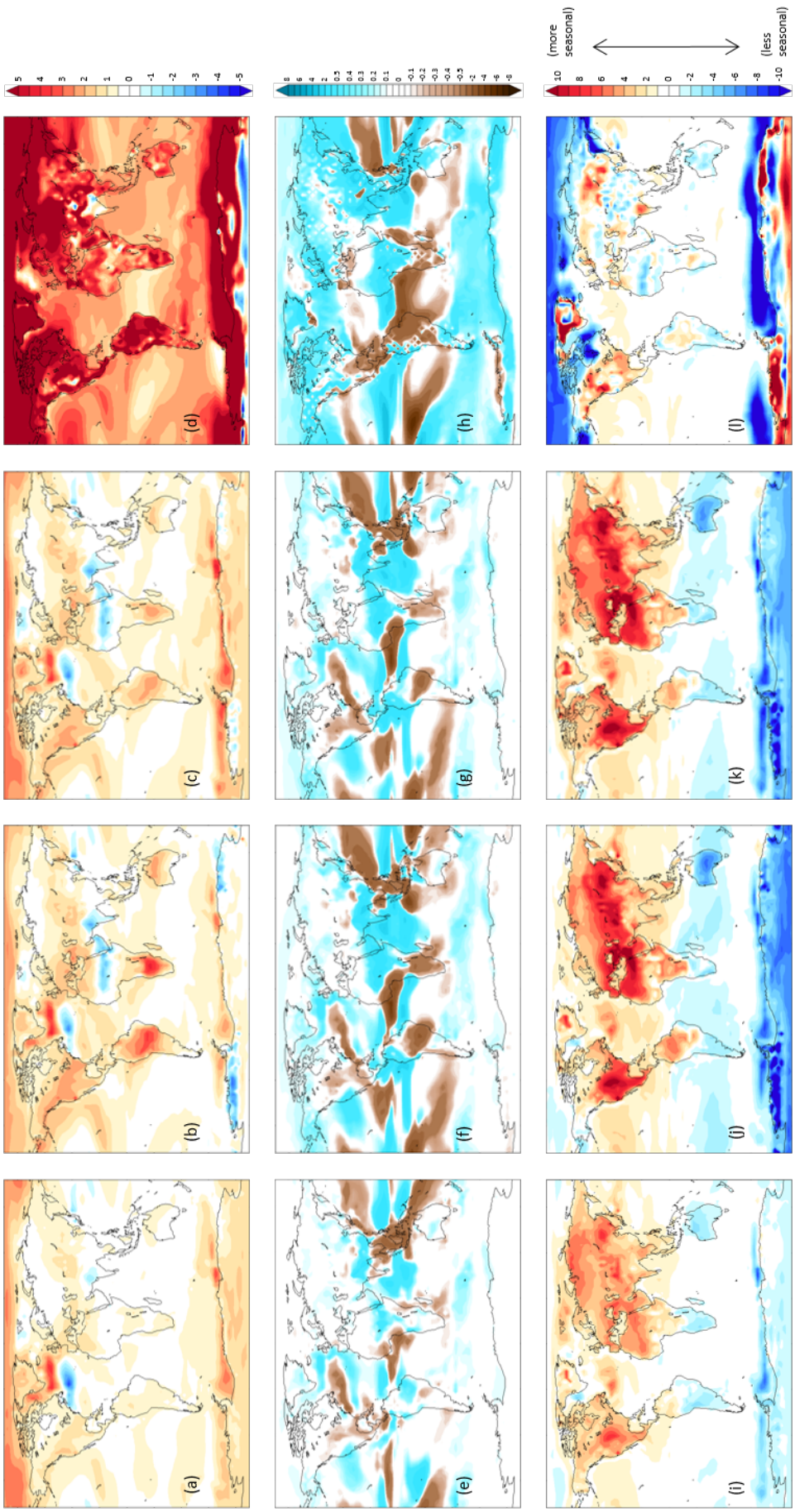
(a)
(b)
(c)
(d)
(e)
(f)
(g)
(h)
(i)
(j)
(k)
(l)
(more seasonal)
(less seasonal)

Figure 2. HadCM3 results run with MOSES1 surface scheme showing (a – d) Annual SAT anomalies (°C) for (a) Plio-G17^{Prescribed} – Plio-KM5c^{Prescribed}, (b) Plio-K1^{Prescribed} – Plio-KM5c^{Prescribed}, (c) Plio-KM3^{Prescribed} – Plio-KM5c^{Prescribed}, (d) Plio-KM5c^{Prescribed} – Pre-Ind^{Prescribed}. (e – h) Annual precipitation anomalies (mm/day) for (e) G17^{Prescribed} – Plio-KM5c^{Prescribed}, (f) Plio-K1^{Prescribed} – Plio-KM5c^{Prescribed}, (g) Plio-KM3^{Prescribed} – Plio-KM5c^{Prescribed}, (h) Plio-KM5c^{Prescribed} – Pre-Ind^{Prescribed}. (i – l) Seasonal range surface temperature anomalies (°C); each figure shows warm monthly mean minus cold monthly mean minus the same for the control. (i) Plio-G17^{Prescribed} – Plio-KM5c^{Prescribed}, (j) Plio-K1^{Prescribed} – Plio-KM5c^{Prescribed}, (k) Plio-KM3^{Prescribed} – Plio-KM5c^{Prescribed}, (l) Plio-KM5c^{Prescribed} – Pre-Ind^{Prescribed}.

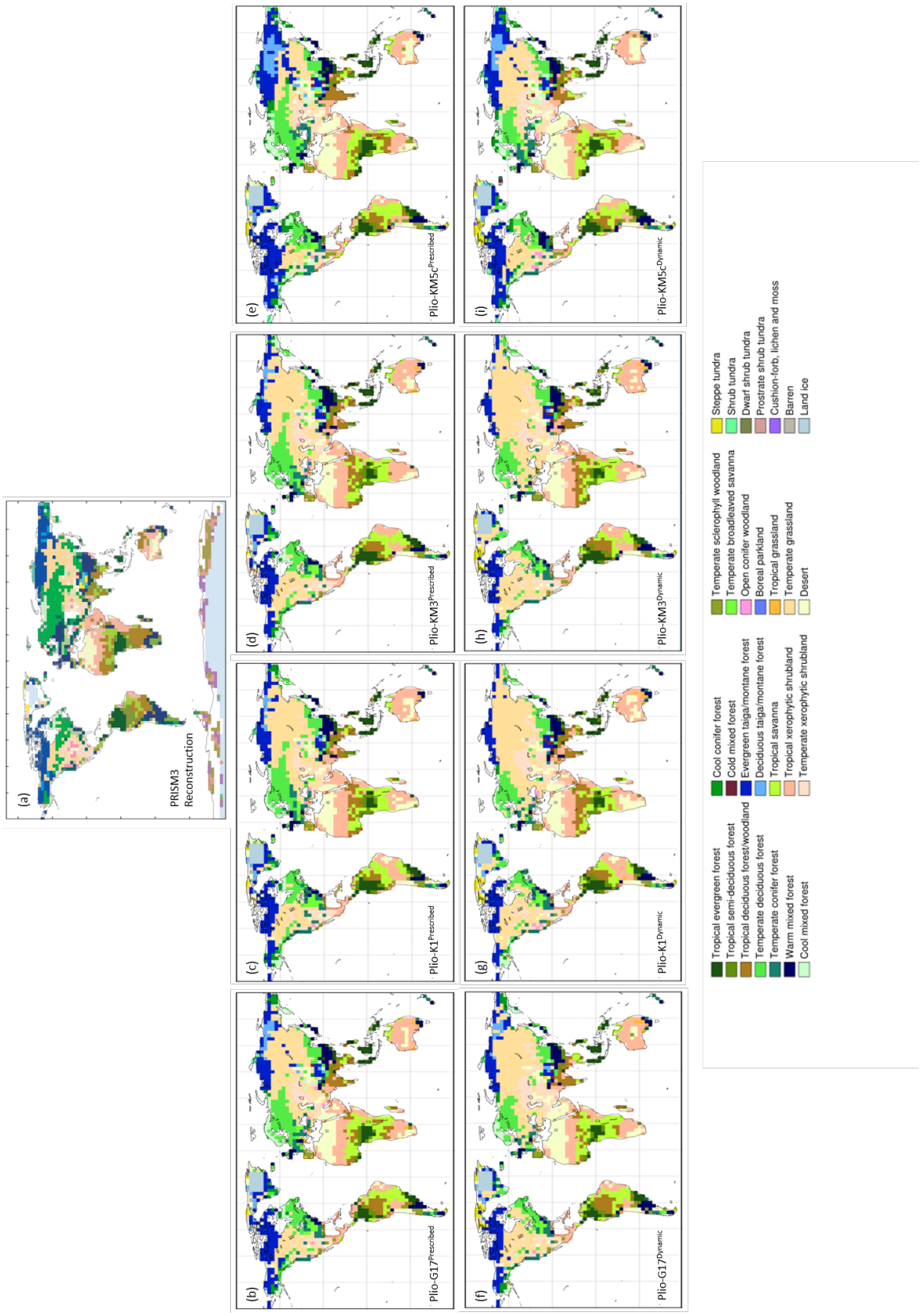

Figure 3. (a) Modelled PRISM3 vegetation reconstruction run with BIOME4 from Salzmann et al. (2008). (b – E) Global Pliocene predicted biomes simulated by BIOME4 with experiments

1021 run with prescribed vegetation with HadCM3 and land surface scheme MOSES1. (f – i) Global
1022 Pliocene predicted biomes simulated by BIOME4 with experiments run with HadCM3 coupled
1023 to TRIFFID vegetation model and Land surface scheme MOSES2. Note the larger expanse of
1024 grassland throughout Asia, especially with experiments where vegetation was allowed to run
1025 dynamically (f – i).

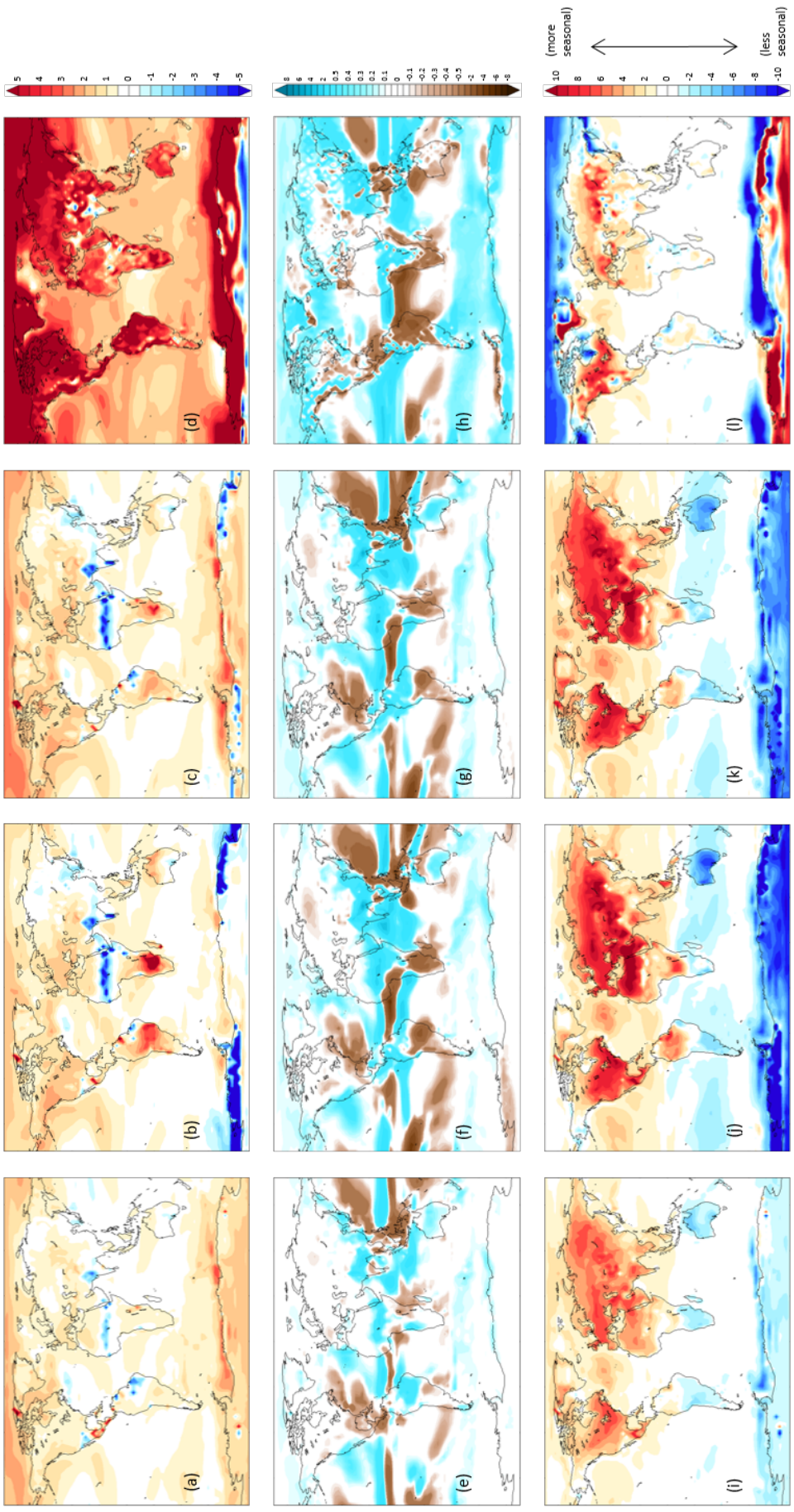
(a)
(b)
(c)
(d)
(e)
(f)
(g)
(h)
(i)
(j)
(k)
(l)
(more seasonal)
(less seasonal)

Figure 4. HadCM3 results run with MOSES2 surface scheme showing (a – d) Annual SAT anomalies (°C) for (a) Plio-G17^{Dynamic} – Plio-KM5c^{Dynamic}, (b) Plio-K1^{Dynamic} – Plio-KM5c^{Dynamic}, (c) Plio-KM3^{Dynamic} – Plio-KM5c^{Dynamic}, (d) Plio-KM5c^{Dynamic} – Pre-Ind^{Dynamic}. (e – h) Annual precipitation anomalies (mm/day) for (e) G17^{Dynamic} – Plio-KM5c^{Dynamic}, (f) Plio-K1^{Dynamic} – Plio-KM5c^{Dynamic}, (g) Plio-KM3^{Dynamic} – Plio-KM5c^{Dynamic}, (h) Plio-KM5c^{Dynamic} – Pre-Ind^{Dynamic}. (i – l) Seasonal range surface temperature anomalies (°C); each figure shows warm monthly mean minus cold monthly mean minus the same for the control. (i) Plio-G17^{Dynamic} – Plio-KM5c^{Dynamic}, (j) Plio-K1^{Dynamic} – Plio-KM5c^{Dynamic}, (k) Plio-KM3^{Dynamic} – Plio-KM5c^{Dynamic}, (l) Plio-KM5c^{Dynamic} – Pre-Ind^{Dynamic}.

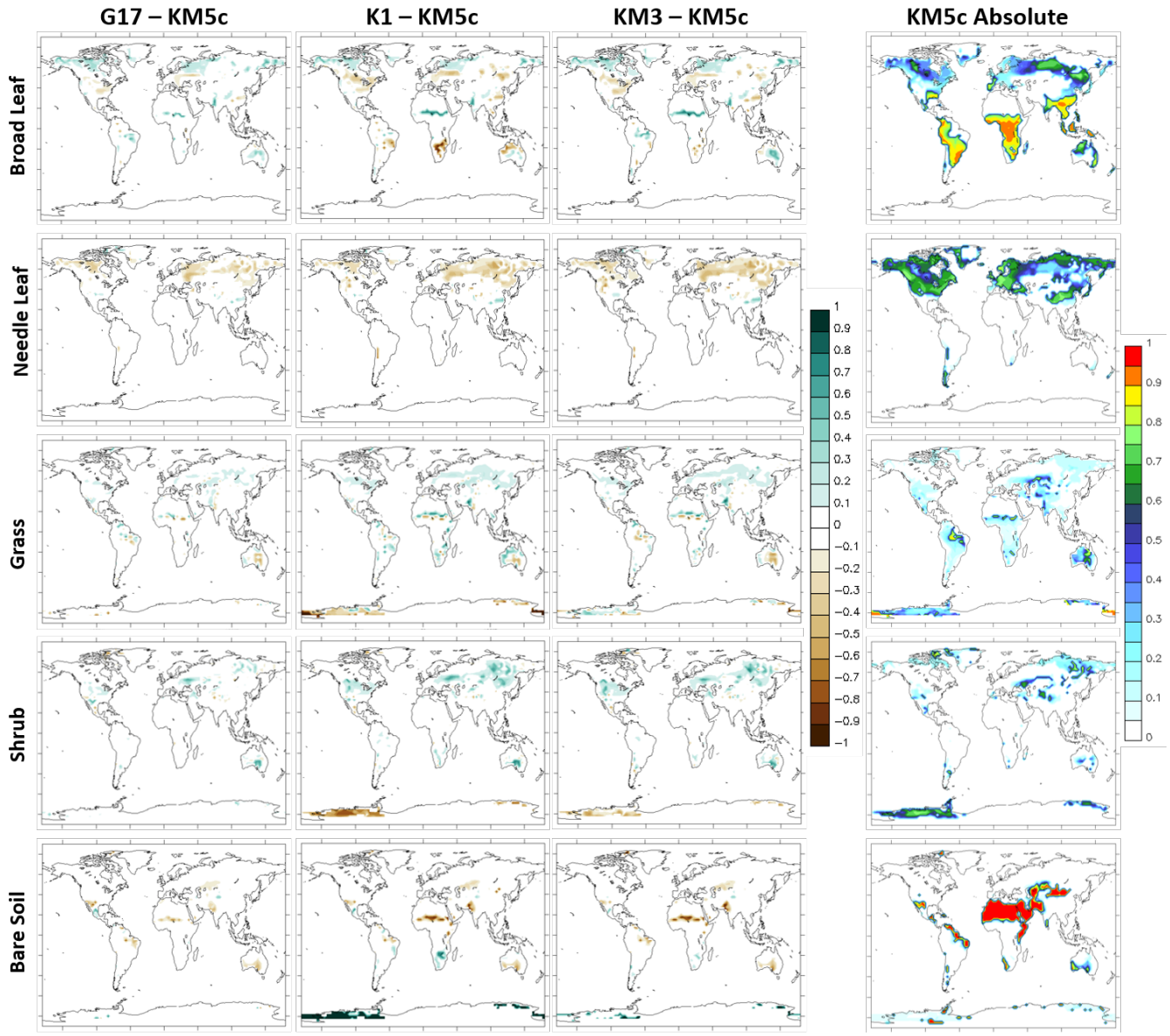

Figure 5. Model predictions experiments run with dynamic vegetation for TRIFFID predicted Plant Functional Types (PFTs) shown as percentage anomalies from control run MIS KM5c (Plio-KM5c^{Dynamic}) for (left) Plio-G17^{Dynamic} – Plio-KM5c^{Dynamic}; (middle-left) Plio-K1^{Dynamic} – Plio-KM5c^{Dynamic}; (middle-right) Plio-KM3^{Dynamic} – Plio-KM5c^{Dynamic}; (right) Control Plio-KM5c^{Dynamic} absolute plant functional types.

Table:

Experiment name	Land Surface Scheme	Vegetation	Orbit	Eccentricity	Precession	Obliquity	MAT °C	MAP mm/day	JJA °C	DJF °C	JJA mm/day	DJF mm/day
Plio-G17^{Dynamic}	MOSES 2.1	Dynamic	2950	0.04	-0.01776	23.96	19.35	3.044	22.45	16.35	3.102	2.990
Plio-K1^{Dynamic}	MOSES 2.1	Dynamic	3060	0.05	-0.05086	23.01	19.35	3.035	22.95	16.05	2.954	3.111
Plio-KM3^{Dynamic}	MOSES 2.1	Dynamic	3155	0.05	-0.04350	23.76	19.45	3.022	23.15	16.15	3.005	3.023
Plio-KM5c^{Dynamic}	MOSES 2.1	Dynamic	3205	0.01	0.00605	23.47	18.85	3.011	21.25	16.55	3.058	2.980
Pre-Ind^{Dynamic}	MOSES 2.1	Dynamic	Pre-Ind	0.02	0.01628	23.44	14.85	2.907	17.15	13.05	2.982	2.867
Plio-G17^{Prescribed}	MOSES 1	Prescribed	2950	0.04	-0.01776	23.96	18.55	3.095	21.25	15.85	3.183	3.015
Plio-K1^{Prescribed}	MOSES 1	Prescribed	3060	0.05	-0.05086	23.01	18.75	3.099	21.85	15.85	3.065	3.112
Plio-KM3^{Prescribed}	MOSES 1	Prescribed	3155	0.05	-0.04350	23.76	18.75	3.108	21.85	15.75	3.132	3.071
Plio-KM5c^{Prescribed}	MOSES 1	Prescribed	3205	0.01	0.00605	23.47	18.05	3.059	20.05	15.95	3.144	2.997
Pre-Ind^{Prescribed}	MOSES 1	Prescribed	Pre-Ind	0.02	0.01628	23.44	13.85	2.877	15.65	11.95	2.964	2.833

Table 1. Summary of experiments including orbital parameters implemented in HadCM3, also showing global mean annual and seasonal temperatures and precipitation. Control experiments indicated in bold.

Supplementary Figures:

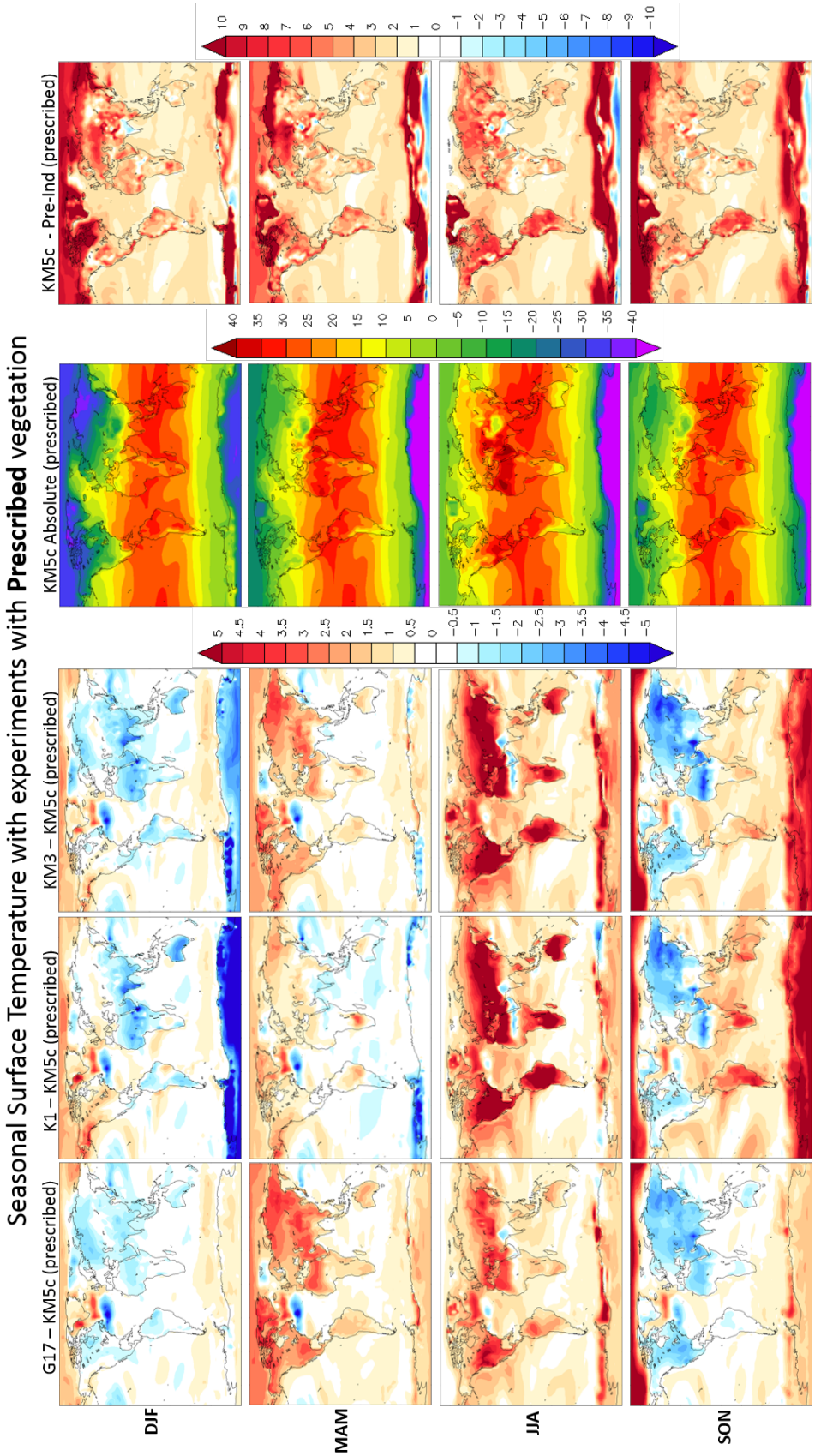
Seasonal Surface Temperature with experiments with **Prescribed** vegetation
G17 – KM5c (prescribed)
K1 – KM5c (prescribed)
KM3 – KM5c (prescribed)
KM5c Absolute (prescribed)
KM5c - Pre-Ind (prescribed)
DJF
MAM
JJA
SON

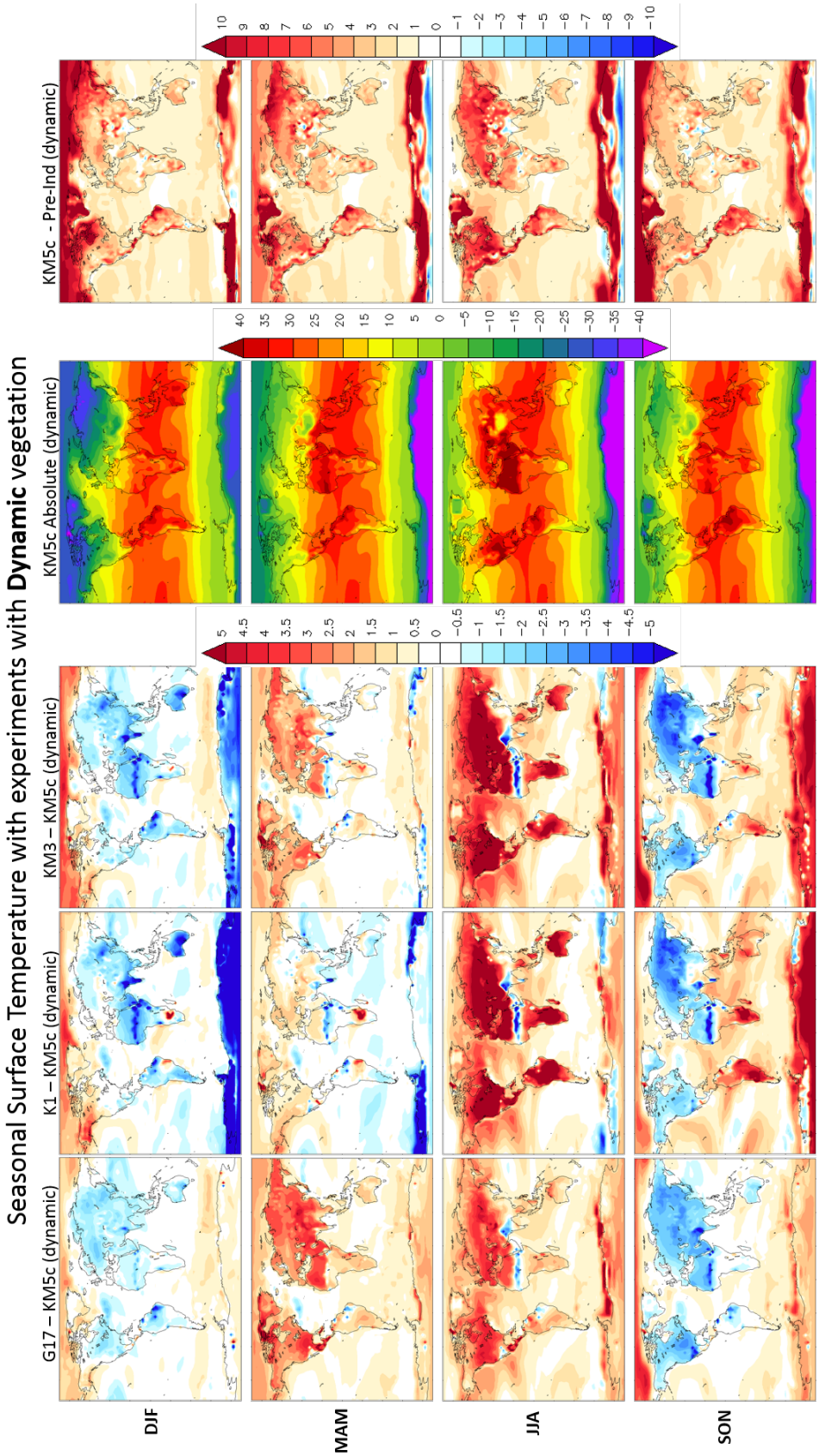
Seasonal Surface Temperature with experiments with Dynamic vegetation
G17 – KM5c (dynamic)
K1 – KM5c (dynamic)
KM3 – KM5c (dynamic)
KM5c Absolute (dynamic)
KM5c - Pre-Ind (dynamic)
DJF
MAM
JJA
SON

1054

1055

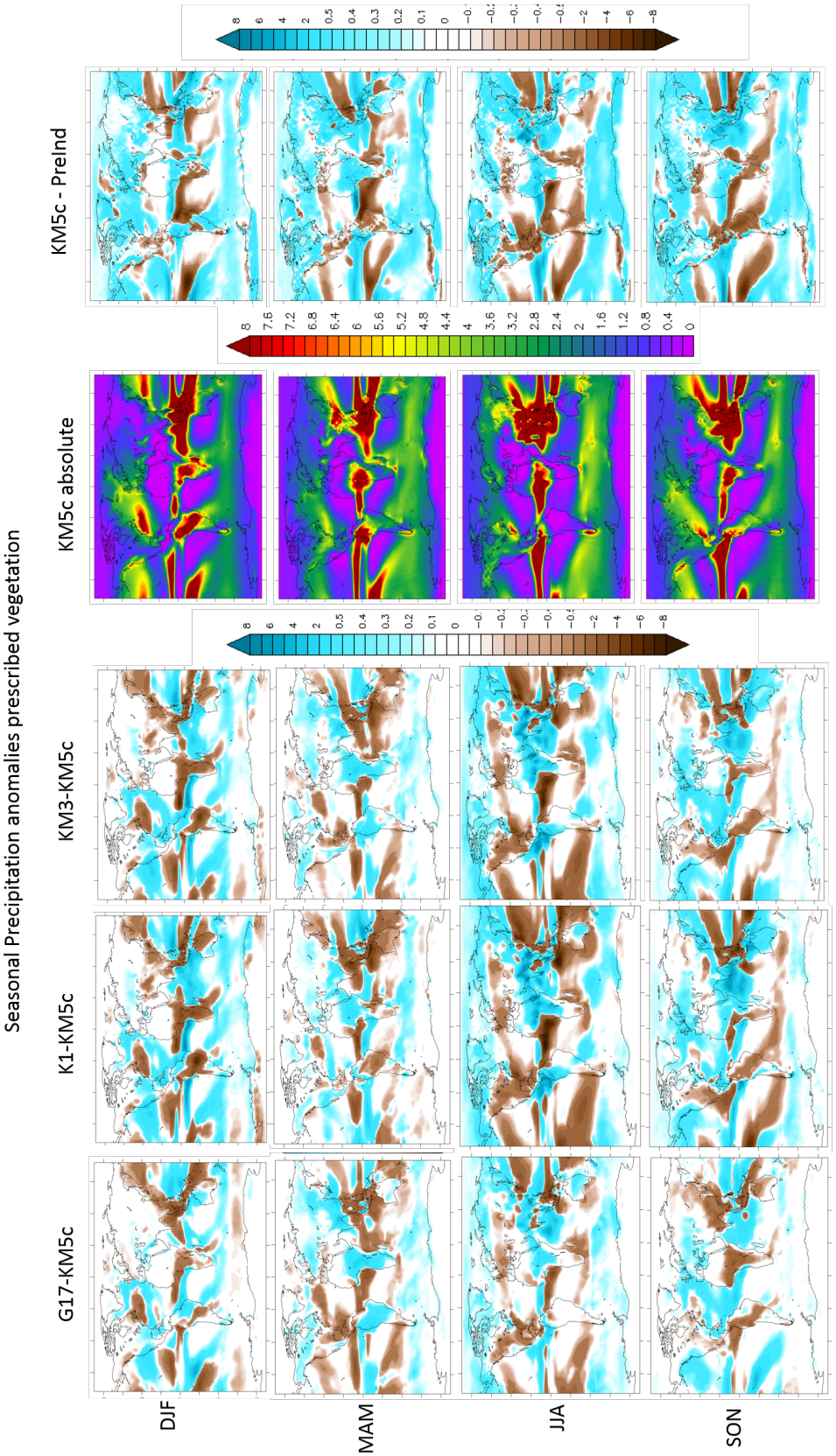
Seasonal Precipitation anomalies prescribed vegetation
G17-KM5c
K1-KM5c
KM3-KM5c
KM5c absolute
KM5c - PreInd
DJF
MAM
JJA
SON

1056

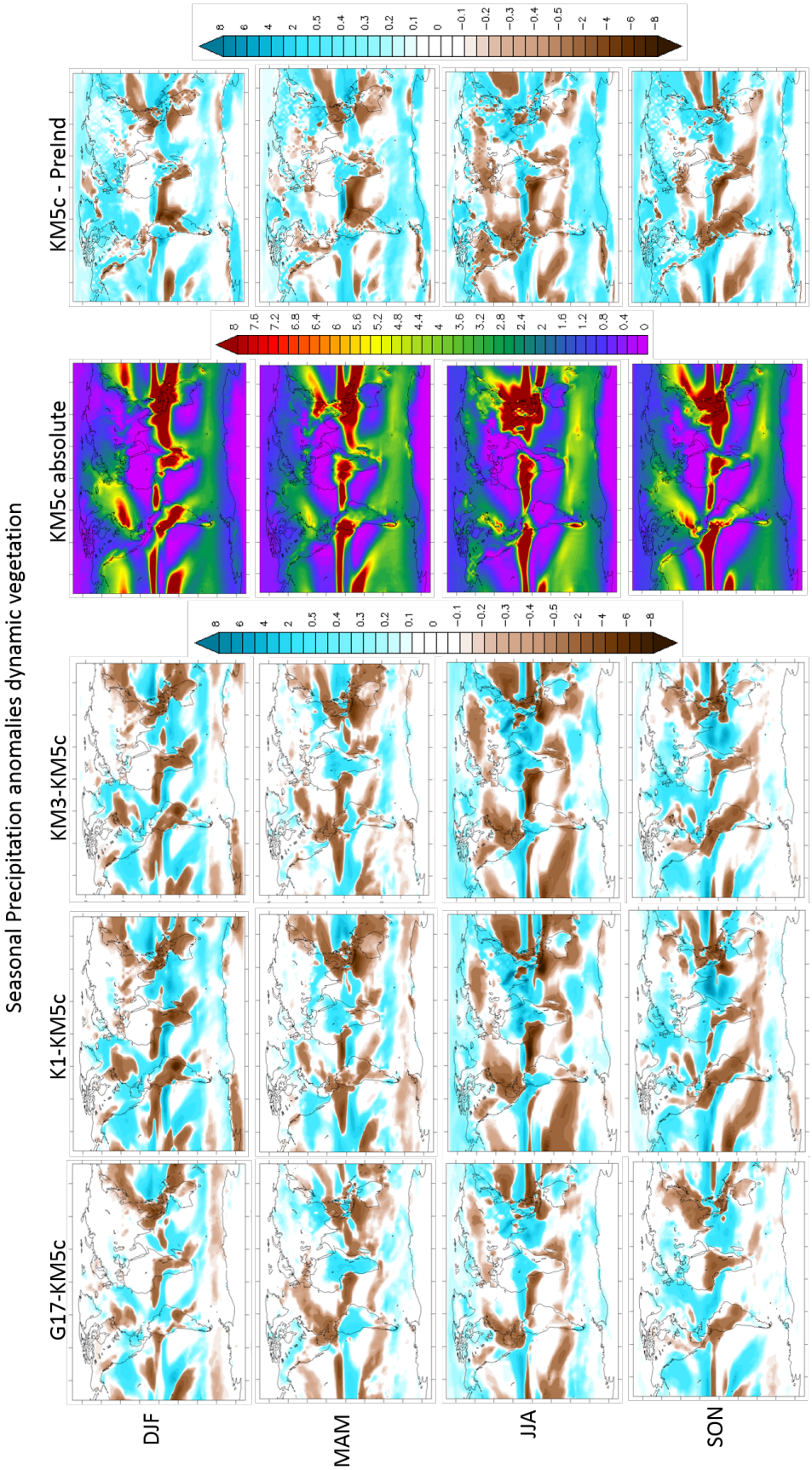
Seasonal Precipitation anomalies dynamic vegetation
G17-KM5c
K1-KM5c
KM3-KM5c
KM5c absolute
KM5c - PreInd
DJF
MAM
JJA
SON

1057

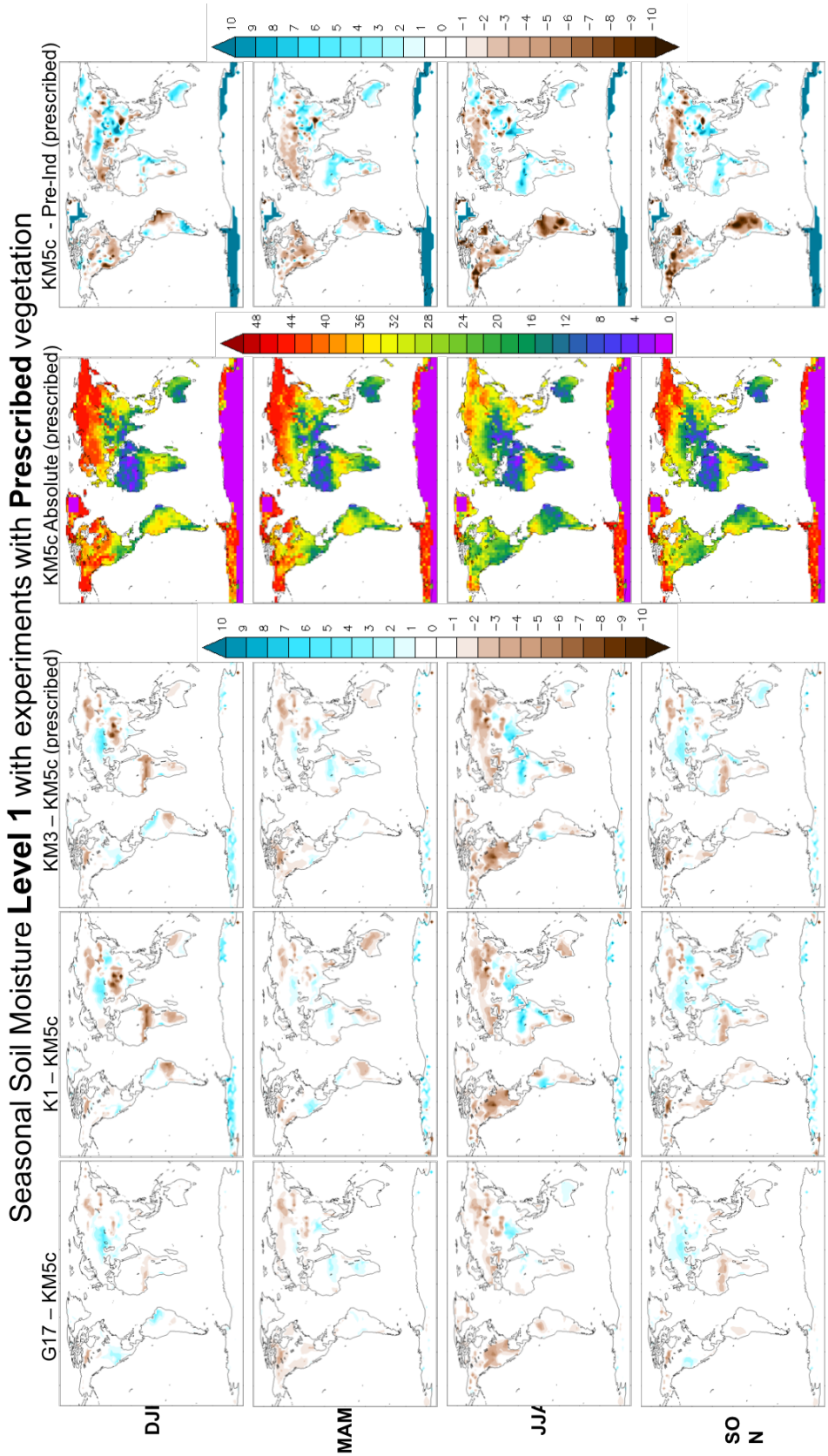
Seasonal Soil Moisture Level 1 with experiments with Prescribed vegetation
G17 – KM5c
K1 – KM5c
KM3 – KM5c (prescribed)
KM5c Absolute (prescribed)
KM5c - Pre-Ind (prescribed)
DJF
MAM
JJA
SON

1058

1059

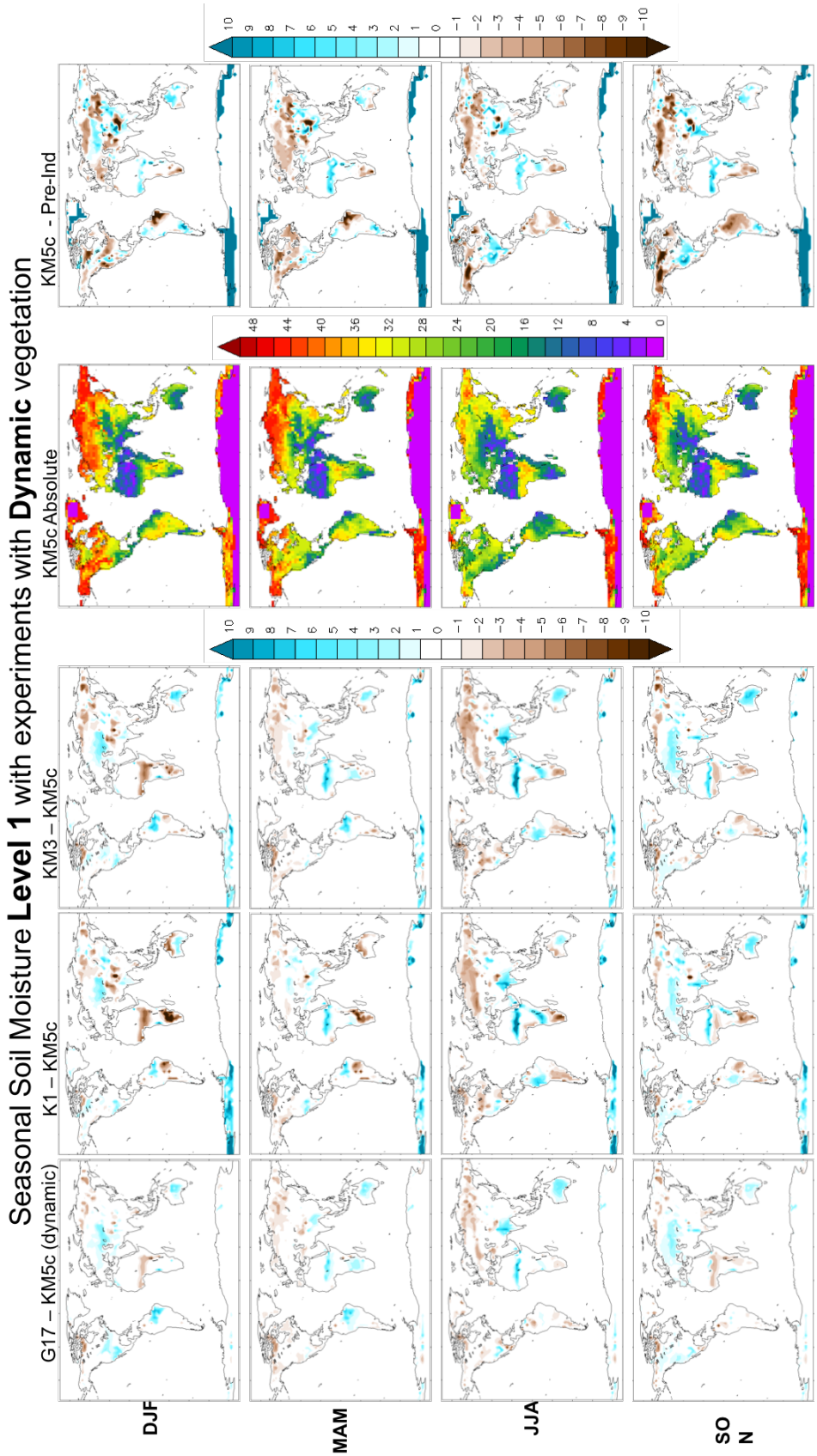
Seasonal Soil Moisture Level 1 with experiments with Dynamic vegetation
G17 – KM5c (dynamic)
K1 – KM5c
KM3 – KM5c
KM5c Absolute
KM5c - Pre-Ind
DJF
MAM
JJA
SON

1060

1061

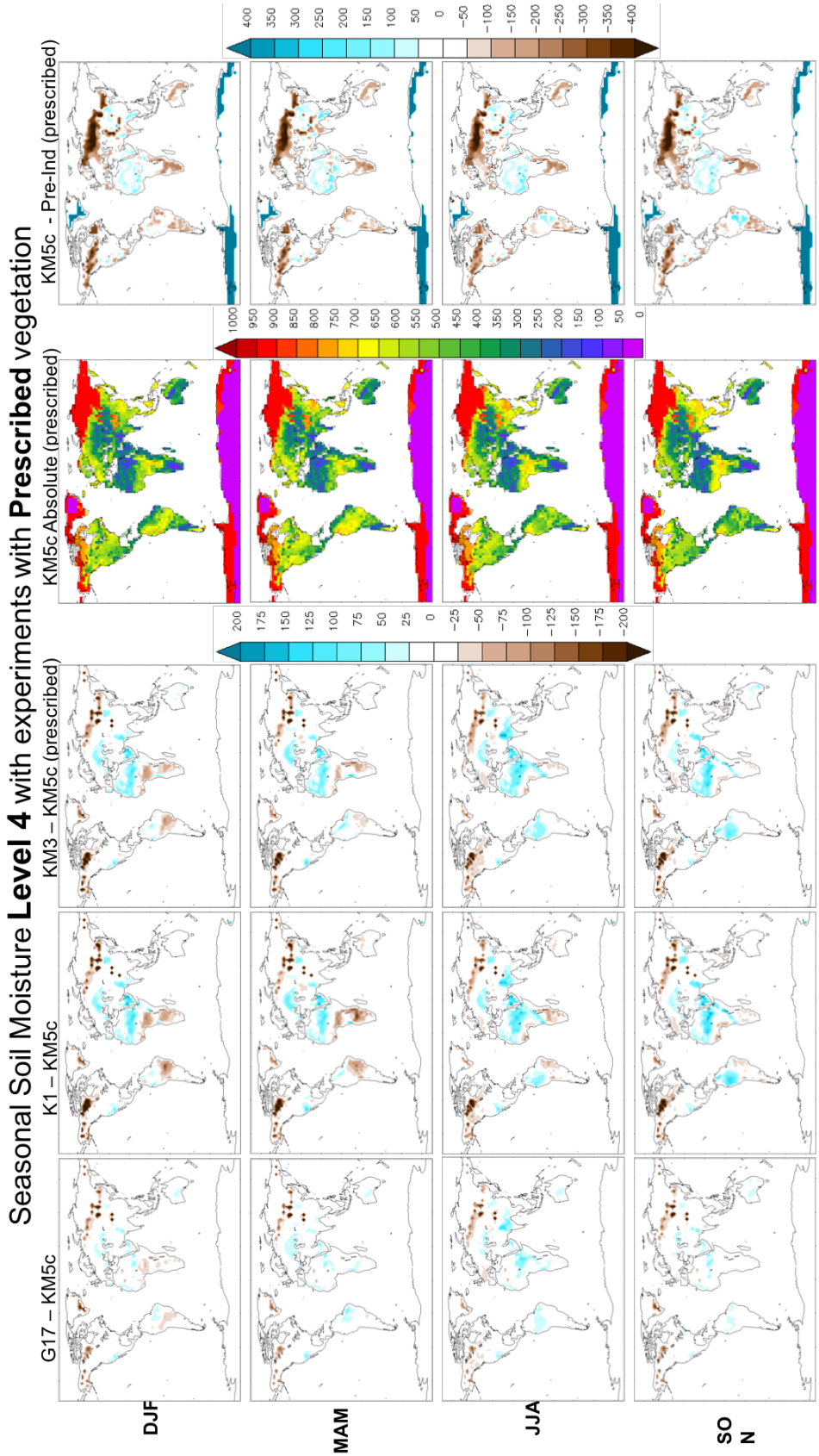
Seasonal Soil Moisture Level 4 with experiments with Prescribed vegetation
G17 – KM5c
K1 – KM5c
KM3 – KM5c (prescribed)
KM5c Absolute (prescribed)
KM5c - Pre-Ind (prescribed)
DJF
MAM
JJA
SON

1062

1063

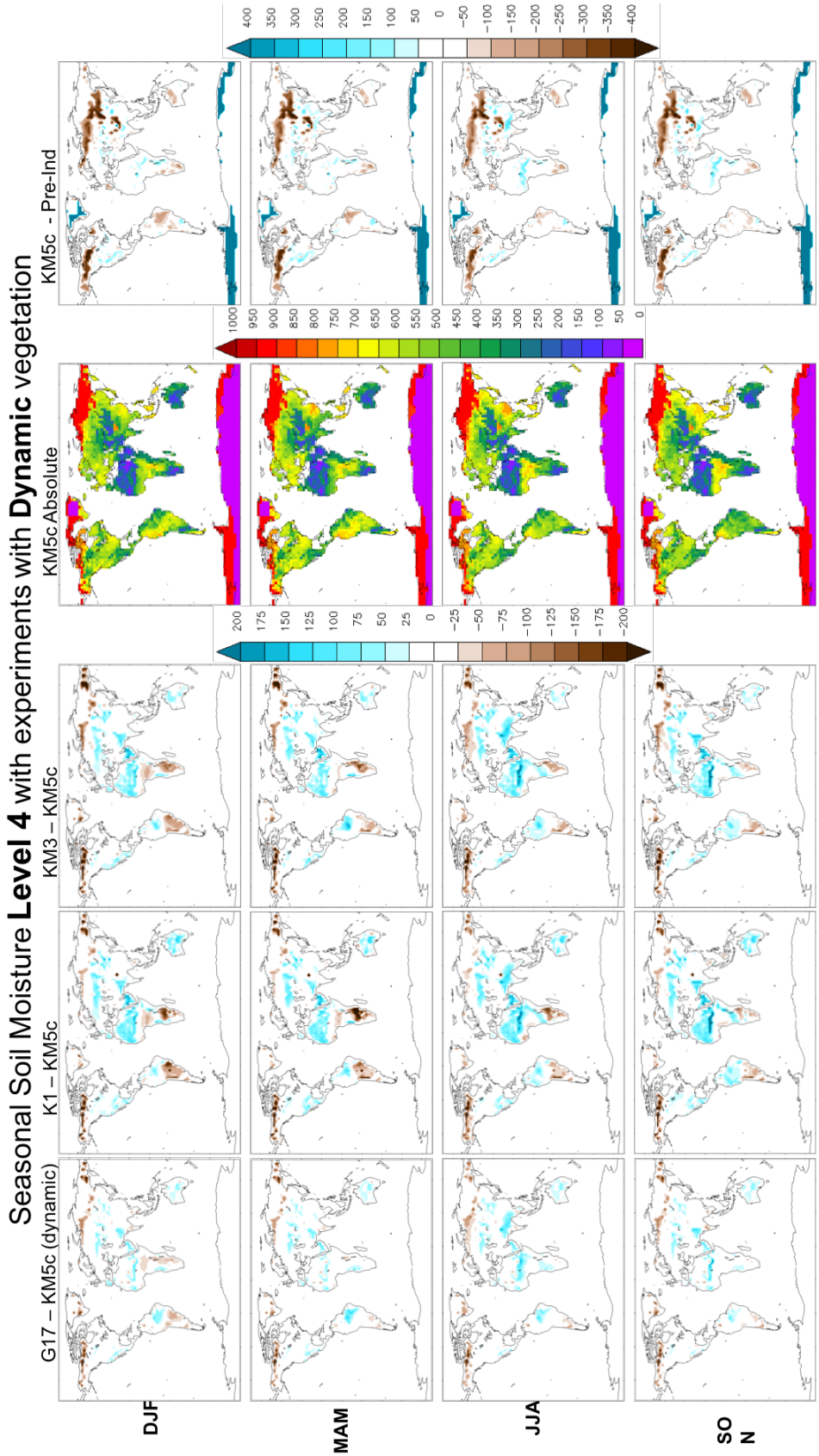
Seasonal Soil Moisture Level 4 with experiments with Dynamic vegetation
G17 – KM5c (dynamic)
K1 – KM5c
KM3 – KM5c
KM5c Absolute
KM5c - Pre-Ind
DJF
MAM
JJA
SON

1064

1065

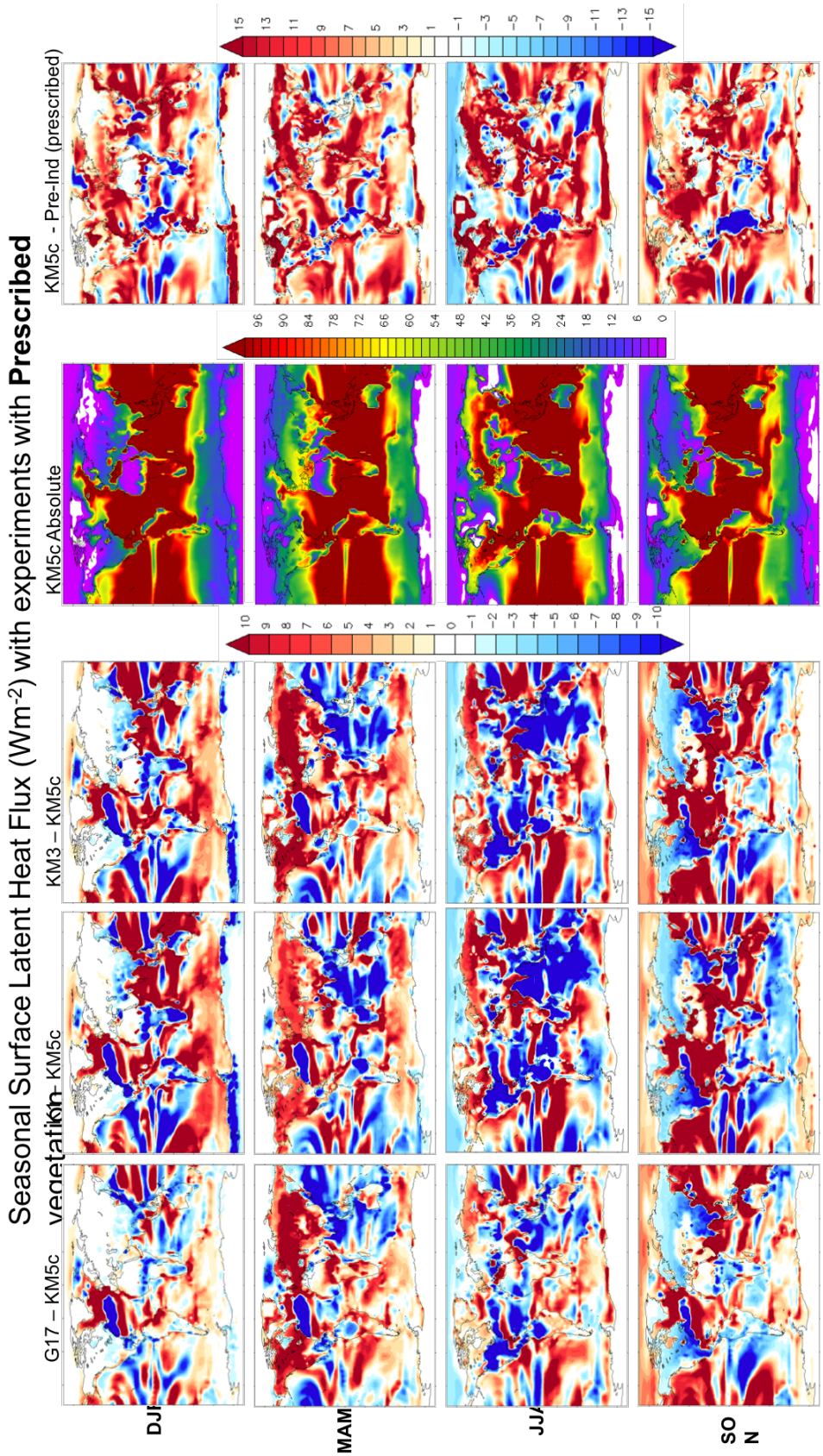
Seasonal Surface Latent Heat Flux (Wm-2) with experiments with Prescribed
G17 – KM5c
KM3 – KM5c
KM5c Absolute
KM5c - Pre-Ind (prescribed)
DJF
MAM
JJA
SON

1066

1067

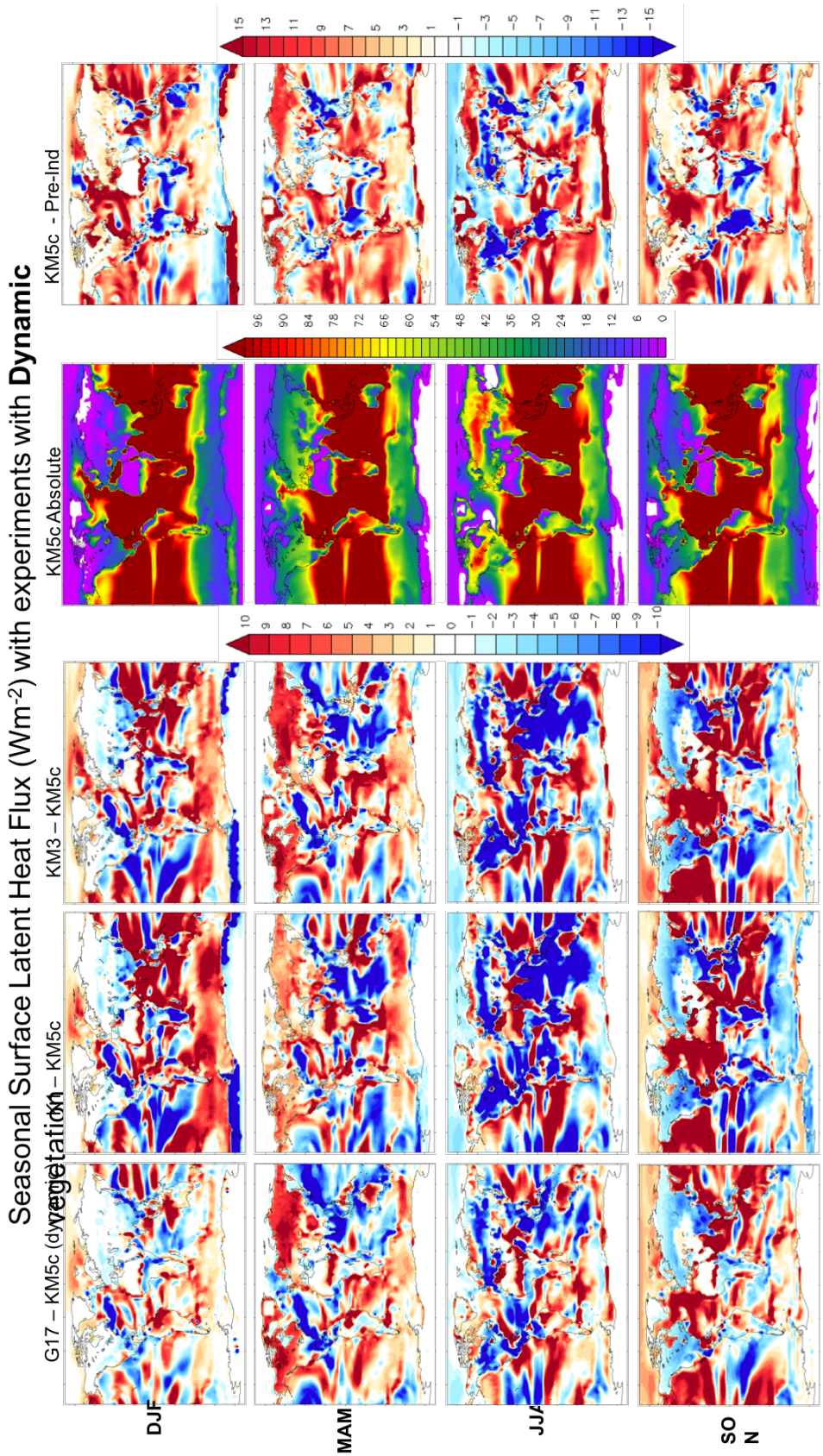
Seasonal Surface Latent Heat Flux (Wm-2) with experiments with Dynamic vegetation
G17 – KM5c (dynamic)
KM1 – KM5c
KM3 – KM5c
KM5c Absolute
KM5c - Pre-Ind
DJF
MAM
JJA
SON

1068

Cover Letter, for Editor only

Caroline Prescott

Sellwood Group for Palaeoclimatology.
School of Earth and Environment
University of Leeds
Leeds, LS2 9JT, UK
Email: js07c2lp@leeds.ac.uk

28.07.2016

Dear Sir/Madam,

Please find attached the manuscript entitled "Regional Climate and Vegetation Change during Interglacial Events within the mid-Pliocene Warm Period" by C.L. Prescott, A.M. Dolan, A. M. Haywood, S. J. Hunter, J.C. Tindall and S.J. Pickering that we herewith submit for publication as a research paper in the journal *Palaeogeography, Palaeoclimatology, Palaeoecology*.

The mid-Pliocene Warm Period (mPWP; 3.264-3.025 Ma) is a recognised valuable target for environmental reconstruction and modelling in order to understand climate and environmental processes in a warmer-than-modern world. However, the nature of climate and environmental variability on orbital timescales during the mPWP remains poorly constrained. We therefore use climate model simulations to analyse mPWP vegetation cover and how this varies between four distinct, and particularly pronounced, interglacial events during the mPWP (Marine Isotope Stages (MIS) G17, K1, KM3 and KM5c)). We also assess climate feedbacks associated with the changes in vegetation. We discuss the orbitally forced simulated vegetation in comparison with published vegetation reconstructions.

This manuscript is an original contribution, and it is not under consideration by another journal. We hope that you will find the paper both interesting and worthy of being published in *Palaeogeography, Palaeoclimatology, Palaeoecology*.

We thank you very much for considering our manuscript,

Yours Sincerely,

Caroline Prescott
PhD student University of Leeds